

R. F. CASTEN, P. KLEINHEINZ, P. J. DALY AND B. ELBEK

A STUDY OF ENERGY LEVELS
AND CORIOLIS COUPLING IN ODD-MASS
WOLFRAM NUCLEI BY MEANS OF
 (d,p) AND (d,t) REACTIONS

Det Kongelige Danske Videnskabernes Selskab
Matematisk-fysiske Meddelelser 38, 13



Kommissionær: Munksgaard
København 1972

CONTENTS

	Page
1. Introduction	3
2. Theoretical considerations	4
3. Experimental procedure and results	7
3.1. Experimental techniques	7
3.2. Spectra and cross section tables	7
3.3. Cross section normalization and error assignments	8
3.4. <i>Q</i> -reduction and DWBA calculations	16
3.5. Cross section angular distributions and <i>l</i> -values	18
3.6. Ground state <i>Q</i> -values	20
4. Nilsson assignments	20
4.1. The 7/2 - [514] orbital	24
4.2. The 1/2 - [521] orbital	25
4.3. The 5/2 - [512] orbital	26
4.4. The 1/2 - [510] orbital	26
4.5. The 3/2 - [512] orbital	27
4.6. The 7/2 - [503] orbital	28
4.7. The 9/2 - [505] orbital	29
4.8. The <i>N</i> = 6 orbitals from the $i_{13/2}$ shell	31
4.9. Higher-lying particle excitations	35
4.10. Comparison of experimental and calculated transfer strengths	38
4.11. Single particle level schemes	39
5. Coriolis coupling of the <i>N</i> = 5 orbitals	40
5.1. Methods of calculation	41
5.2. Fermi surface location	42
5.3. Empirical Coriolis coupling strength	44
5.4. Analysis of results for Coriolis coupled bands	47
6. Conclusions	55
Appendix	57

Synopsis

The energy levels of ^{170}W , ^{181}W , ^{188}W , ^{185}W and ^{187}W have been investigated by means of (*d,p*) and (*d,t*) reactions. The deuteron energy was 12.1 MeV and the charged reaction products were analyzed in a magnetic spectrograph at 60°, 90° and 125°. The results established detailed level schemes and greatly improved the understanding of the level structure in these nuclei. All the *N* = 5 Nilsson orbitals in an energy range of about 4 MeV have been identified. In addition, several *N* = 6 ($i_{13/2}$) Nilsson states have been located by combining the present results with those of a concurrent ($^3\text{He},\alpha$) reaction study. A quantitative analysis of the Coriolis coupling of the *N* = 5 orbitals was performed. It was found that many gross discrepancies between the experimental cross sections and those calculated using the Nilsson model and the distorted-wave Born approximation could be eliminated or reduced by inclusion in the cross section calculations of the Coriolis interaction with reduced coupling matrix elements. In particular, the highly distinctive systematics of the cross sections in different isotopes could be reproduced. An energy-dependent systematic reduction of the matrix elements which satisfactorily accounts for most of the experimental observations is suggested.

1. Introduction

This investigation continues a series¹⁻⁴⁾ performed in this laboratory in the past few years. The previous work has investigated several deformed rare earth nuclei by means of the (d,p) and (d,t) reactions. The location and properties of single particle neutron states and the rotational bands built on them have been studied in a systematic manner. The results have demonstrated that the simple Nilsson model, with pairing, coupled to a standard set of DWBA calculations is quite successful as a tool for the interpretation of low-lying levels in deformed nuclei. Certain deviations from this simple scheme, such as the mixing of single-particle states or the coupling to collective excitations, were also qualitatively considered.

The present investigation continues this program with a study of the odd wolfram nuclei. In addition, a quantitative analysis is presented here of the Coriolis mixing⁵⁾ among the Nilsson orbitals and its effects on energies and cross sections. This mixing sometimes alters energies by as much as a few hundred keV and cross sections by orders of magnitude. The presence of Coriolis mixing is frequently manifested by the occurrence of widely varying inertial parameters of the different rotational bands. Accordingly, one test of the adequacy of a mixing analysis is that inertial parameters for the unperturbed bands should approach both each other and the neighbouring even-even nucleus value. Coriolis coupling often can significantly alter the expected relative population cross sections for the successive levels of a rotational band. In such cases, this so-called finger-print pattern becomes unrecognizable and hence the direct orbital identification difficult. In the present investigation a large number of such deviations from the simple Nilsson scheme could be accounted for with the inclusion of the Coriolis interaction. It has been frequently found⁵⁻¹⁰⁾ that the Coriolis matrix elements predicted from the Nilsson model are inadequate and need to be adjusted empirically in order to fit the experimental results. The present data also require such adjustments, and an investigation has been made of the properties of the basic strength of the Coriolis interaction.

The data obtained by the (d,t) reaction have been supplemented by a study of the $({}^3\text{He},\alpha)$ reaction which, at an angle of 60° , preferentially populates hole states requiring high orbital angular momentum transfer. This is the case for the $N = 6$ states originating from the $i_{13/2}$ spherical shell model state. Their associated rotational bands have nearly all their strength in the $I = 13/2 +$ members. Despite having, therefore, no easily recognizable fingerprint pattern, their identification is rendered much easier with the combination of the $({}^3\text{He},\alpha)$ and (d,t) reactions. The analysis of the $({}^3\text{He},\alpha)$ studies is being published separately¹¹⁾ although the main results will be cited here for completeness.

Previous studies by ERSKINE and SIEMSEN¹²⁻¹⁴⁾ of ${}^{183}\text{W}$, ${}^{185}\text{W}$ and ${}^{187}\text{W}$ using the (d,p) reaction alone located several low-lying Nilsson orbitals in these nuclei and showed that the observed transfer cross sections could be satisfactorily explained by including the Coriolis interaction in the theoretical cross section calculations. Our results are in general agreement with these earlier findings.

2. Theoretical considerations

The simple equations describing the transfer reactions studied here as well as those concerning the Coriolis interaction have been given elsewhere¹⁵⁾. We shall partly repeat them to establish a notation and terminology for the discussion to follow.

In the special case of a single-neutron stripping or pickup reaction on an even-even spin-zero target proceeding by a single step process to a state of spin $I = j$ of a rotational band built on a given Nilsson orbital, the differential cross section may be written as the product of the intrinsic cross section for the neutron transfer with orbital angular momentum l , the C_{jl}^2 coefficient characterizing the Nilsson orbital, and a pairing factor P :

$$\frac{d\sigma}{d\Omega}(\theta) = 2\varphi_l(\theta) \cdot C_{jl}^2 \cdot P^2 \quad (1)$$

where $j = l \pm \frac{1}{2}$. The intrinsic reaction cross section $\varphi_l(\theta)$ for the specified reaction is the normalized DWBA cross section

$$\varphi_l(\theta) = N^{(\pm)} \cdot \sigma_l^{DWBA}(\theta) \quad (2)$$

The $\sigma_l(\theta)$ are calculated once, for all l -values and for both the (d,p) and (d,t) reactions by a standard DWBA code. The normalization factors are taken as $N^{(+)} = 1.5$ for the (d,p) and $N^{(-)} = 3.0$ for the (d,t) reaction.

The C_{jI} factors are the expansion coefficients of the Nilsson wave functions on a basis of spherical wave functions. Any pure Nilsson orbital is specified by a set of these coefficients from $C_{j=K,l}$ to $C_{j=N+\frac{1}{2},l}$, N here being the principal quantum number of the Nilsson orbital and K the angular momentum projection on the nuclear symmetry axis; l and N are of equal parity. This sequence of coefficients gives, by eq. (1), the relative transfer cross sections into the successive members of a rotational band, called a "fingerprint pattern", which is used as a tool for identification of such orbitals.

The factor P in eq. (1) is the occupation amplitude, U or V , for a stripping or pickup reaction, respectively. It is assumed to be constant for the various rotational members of a band. According to the pairing theory, it may be calculated from the gap parameter Δ and the excitation energy E of the band head ($I = K$) by the relations

$$E = \sqrt{(\varepsilon - \lambda)^2 + \Delta^2} - \sqrt{(\varepsilon_0 - \lambda)^2 + \Delta^2} \quad (3)$$

and

$$P^2 = \left\{ \frac{U^2}{V^2} \right\} = \frac{1}{2} \left(1 \pm \frac{\varepsilon - \lambda}{\sqrt{(\varepsilon - \lambda)^2 + \Delta^2}} \right). \quad (4)$$

Here, ε is the single particle Nilsson energy, with ε_0 being that of the ground state, λ is the energy of the Fermi surface, and Δ is half the energy gap and is taken to be 750 keV from the empirical even-odd mass differences in the wolfram nuclei. Wherever in the interpretation of the data in this work pairing effects are important, they have been calculated from eqs. (3) and (4).

With the inclusion of band mixing, the cross section to a given level is not specified solely by one C_{jI} coefficient but by a set of products, $a_{in} C_{jI}^{(i)}$, of the admixed amplitudes a_{in} of the level i into the level n times the C_{jI} coefficient for the i^{th} orbital. In this case, the cross section becomes

$$\frac{d\sigma_n(\theta)}{d\Omega} = 2\varphi_i(\theta) \cdot \left(\sum_i a_{in} C_{jI}^{(i)} P_i \right)^2. \quad (5)$$

Because of the coherent summation, relatively small admixtures can have drastic effects on the cross sections. In what follows we shall apply eq. (5) to the case of Coriolis mixing.

The collective Hamiltonian involves the Coriolis term which couples an odd particle to the rotational motion

$$V_{PRC} = -\frac{\hbar^2}{2\mathfrak{I}}(J_+j_- + J_-j_+) \quad (6)$$

where \mathfrak{I} is the moment of inertia and J_{\pm} and j_{\pm} are standard angular momentum projection raising and lowering operators connecting states differing by one unit in the K quantum number. In eq. (6), $\hbar^2/2\mathfrak{I}$ plays the role of a basic coupling constant determining the strength of the Coriolis mixing.

With the inclusion of pairing, the full Coriolis matrix element between two states of angular momentum I belonging to bands with projection quantum numbers K and $K+1$, takes the form

$$\left. \begin{aligned} &\langle I, K | V_{PRC} | I, K+1 \rangle = \\ &-\frac{\hbar^2}{2\mathfrak{I}} \eta_K \eta_{K+1} \langle K | j_- | K+1 \rangle \sqrt{(I-K)(I+K+1)} (U_K U_{K+1} + V_K V_{K+1}) \end{aligned} \right\} \quad (7)$$

where

$$\langle K | j_- | K+1 \rangle = \sum_j C_{jl}^K C_{jl}^{K+1} \sqrt{(j-K)(j+K+1)}. \quad (8)$$

Expressions for mixing amplitudes and perturbed energies are given in e.g. ref. ⁵⁾. The last factor in eq. (7), reflecting the effects of pairing, tends to diminish the interaction for states on opposite sides of the Fermi level. The two factors η_K and η_{K+1} are attenuation factors and are equal to unity in the Nilsson model but are included here to allow for any alteration of the matrix elements as may be empirically required. As mentioned above, previous investigations⁵⁻¹⁰⁾ of Coriolis coupling have indeed revealed the need for adjustments (generally reductions) in the matrix elements as calculated from the Nilsson model. The use of two attenuation factors in eq. (7) does not necessarily imply that we ascribe the reduction to the individual wave functions entering the matrix element, which in fact has been previously suggested¹⁶⁾. Alternatively, various authors have speculated that $\hbar^2/2\mathfrak{I}$ is not a constant but an off-diagonal operator⁶⁾ or that the pairing factor does not adequately reflect the effects of the pairing correlations¹⁰⁾. In any case, we have studied the amount of attenuation empirically required without investigating all its possible sources and systematics in detail.

It might be noted here finally that if the mixing amplitudes become large, it is rather meaningless to speak of a given state with quantum numbers $|IK|Nn_zA|$ having certain admixtures from other states. This, in fact, occurs among some $N = 6$ orbitals and one cannot speak of a specific Nilsson orbital occurring at a certain energy, but only of the unperturbed posi-

tions of the various orbitals required to produce, after mixing, the final spectrum of thoroughly mixed states. In the $N = 5$ shell, with which we shall be mainly concerned here, such strong mixing rarely occurs and the states are therefore labelled by the Nilsson quantum numbers corresponding to the largest amplitude in the wave function. The full specification for each state is given by the wave functions tabulated in the appendix.

3. Experimental Procedure and Results

3.1. Experimental Techniques

The experimental techniques resemble very much those of previous studies at this laboratory¹⁻⁴). A 12.08 MeV deuteron beam of intensity from 0.3 to 1 μA was obtained from the Niels Bohr Institute's tandem accelerator. Targets of the four even wolfram isotopes ^{180, 182, 184, 186}W ($\approx 50 \mu g/cm^2$) were prepared by direct deposition with an isotope separator on $\approx 50 \mu g/cm^2$ carbon foil by means of a retardation technique¹⁷). The charging material for the ion source was its own wolfram filament. The isotopic enrichment achieved was $\geq 95\%$ except for the ¹⁸⁰W target which was 65% enriched. The reaction products were analyzed in a broad range magnetic spectrograph. It was possible to record the (d,p) , (d,t) and (d,d') reactions simultaneously in different regions on the photographic plates. Aluminium absorbers were applied for particle discrimination in regions where the different spectra overlapped. The energy resolution, at $\theta = 125^\circ$, was 7 to 8 keV fwhm for the triton spectra, and 10 to 12 keV fwhm for the proton spectra which were recorded in a region of the focal plane where the dispersion is smaller. Measurements on all isotopes were made at 60° , 90° and 125° . The beam current was recorded in a Faraday cup 10 cm behind the target. The total charge per exposure was between 5000 and 60000 μC .

3.2. Spectra and Cross Section Tables

Typical spectra are shown in figs. 1 to 8 for both deuteron-induced reactions on each of the four targets studied. Quantum numbers are indicated for all peaks assigned. Contaminant peaks are labelled with the contaminating nuclide. The $(^3He,\alpha)$ spectra are shown in fig. 9. They clearly demonstrate the selectivity of this reaction. The degree of confidence for each assignment is given in the level-diagram for each nucleus (figs. 10 to 14). Adopted level energies and cross sections as well as Nilsson assign-

TABLE 1. Levels populated in ^{179}W .

Energy keV	Assignment $IK^\pi[Nn_zA]$	Experim. cross sect. (d,t) $\mu\text{b/sr}$ 90°	Q -red. cross sect. (d,t) $\mu\text{b/sr}$ 90°
0	7/2 7/2 - [514]	~3	~3
222*	1/2 1/2 - [521]	183	218
305*	3/2 1/2 - [521]	41	53
318*	5/2 1/2 - [521]	44	58
~390		~5	~6
430*	5/2 5/2 - [512]	9	14
468	13/2 9/2 + [624]†	28	44
508*	7/2 1/2 - [521]	56	90
532*	7/2 5/2 - [512]	115	189
533*	9/2 1/2 - [521]		
~560		~4	~7
689	3/2 1/2 - [510]	11	22
722		6	12
748		11	23
788	5/2 1/2 - [510]	13	27
~816	11/2 1/2 - [521]	~4	~9
~914		~18	~40
958		32	85
1031		7	22
~1073		28	86
~1295		8	34

* Energy from γ -ray measurements.

† 13/2+ assignment suggested by (d,t) cross section angular distribution.

ments are listed in tables 1 to 5. In addition to the measured cross sections, the Q reduced differential cross sections at 90° are included in the same tables (see section 3.4).

3.3. Cross Section Normalization and Error Assignments

Normalization of exposures made on the same target was based on the integrated beam current and, independently, on measurements of elastically scattered deuterons using a monitor counter set at 90° to the incident beam. The absolute cross sections, for each angle, were evaluated from comparison with the sum of elastic and inelastic deuteron cross sections at 12 MeV which were obtained from short exposures (5 to 300 μC) before and after each run. The deuteron cross sections were taken¹⁵⁾ to be 530,

TABLE 2. Levels populated in ^{181}W .

Energy keV	Assignment $IK^\pi [Nn_zA]$	Experimental cross section				Q-reduced cross section		Inferred <i>l</i> -value
		$(d,p) \mu\text{b/sr}$	$(d,t) \mu\text{b/sr}$			$(d,p) \mu\text{b/sr}$	$(d,t) \mu\text{b/sr}$	
			90°	60°	90°			
0	9/2 9/2 + [624]	1.9	9	15	10	3	13	4
113*	11/2 9/2 + [624]		~1.6	~1.6	2.2		~1.5	
250*	13/2 9/2 + [624]	18	12	46	52	27	48	6†
366*	5/2 5/2 - [512]	<1	9	10	10	<2	11	3
385*	1/2 1/2 - [521]	14	233	243	184	20	288	1
409*	7/2 7/2 - [514]	<2	11	19	21	<3	23	3
450*	3/2 1/2 - [521]	96	76	obsc	64	135	~95	(1)
476*	7/2 5/2 - [512]	37	116	191	165	51	246	3
488*	5/2 1/2 - [521]	8	49	82	51	11	107	3
~527	9/2 7/2 - [514]		9	24	34		33	<i>h</i>
529*	3/2 1/2 - [510]	~102				~140		
560*	5/2 1/2 - [510]	122	10	16	17	164	23	3
~611	9/2 5/2 - [512]	<1	<5	3	3	<1	4	
642	7/2 1/2 - [521]	~38	19	46	42	~50	70	3, <i>h</i>
662*	7/2 7/2 - [503]	226	14	29	21	296	45	3
715		<10	7	20	17	<14	33	3
726*	3/2 3/2 - [512]	83	5	7	~5	107	11	1,3
777	11/2 5/2 - [512]		<1	4	6		7	<i>h</i>
807*	5/2 3/2 - [512]	102	2.5	7	5	126	13	1,3
937	7/2 3/2 - [512]	~56			~3	~67		
996	9/2 +, <i>N</i> = 6		14	~24	26		~56	3
~1012			~2	<2	5		<4	
1084			<1	5	10		13	<i>h</i>
1124	13/2 +, <i>N</i> = 6		5	20	32		51	6†
1191		<9	21	43	32	<10	125	3
1252		190	4	9	7	204	27	(3)
~1274			5	8	8		26	3
1318			<3	7	8		22	3, <i>h</i>
1354			11	26	24		92	3
1369			3	6	5		~21	3
1426			8	18	16		72	3
1502				5	4		<20	
1652			~6	16	obsc		88	

*Energy from γ -ray measurements.† *l* = 6 from ($^3\text{He},\alpha$) data.

TABLE 3. Levels populated in ^{183}W .

Energy keV	Assignment $IK^\pi [Nn_zA]$	Experimental cross section						Q-reduced cross section		In- ferred l-value
		$(d,p) \mu\text{b/sr}$			$(d,t) \mu\text{b/sr}$			(d,p) $\mu\text{b/sr}$	(d,t) $\mu\text{b/sr}$	
		60°	90°	125°	60°	90°	125°	90°	90°	
0	1/2 1/2 - [510]	5	6	2.8	9	9	3	8	5	
47*	3/2 1/2 - [510]	280	195	86	304	266	104	264	150	1
99*	5/2 1/2 - [510]	197	151	85	154	177	83	202	103	3
207*	7/2 1/2 - [510]	214	111	65	112	116	51	142	72	1
209*	3/2 3/2 - [512]	129	77	52	37	50	23	96	35	3
292*	5/2 3/2 - [512]	129	77	52	37	50	23	96	35	3
309*	9/2 1/2 - [510]	13	8	15	3	10	9	11	7	h
412*	7/2 3/2 - [512]	92	72	50	40	62	36	87	44	3
453*	7/2 7/2 - [503]	245	238	138	68	98	58	284	72	3
487	13/2 11/2 + [615]	17	30	34	9	35	33	35	26	6†
~553	9/2 3/2 - [512]	<3	4	4	<1	<1.3	1	4	<1	
~596	9/2 7/2 - [503]	2.9	obsc	2.6			1	~3	~1	
623	9/2 9/2 + [624]			1.5	8	16	10	~2	13	4
742	11/2 3/2 - [512]	<5	4	5		1.4	2.8	4	1.3	h
906	5/2 5/2 - [512]	5	5	1.9	10	18	11	6	19	3,1
936	1/2 1/2 - [521]	38	15	11	285	342	158	15	364	1
960	13/2 9/2 - [624]				11	38	29		41	6†
1002	7/2 5/2 - [512]	38	29	17	112	207	128	29	237	3
1029	3/2 1/2 - [521]	3	2.7	1.2	45	46	27	2.6	54	1
1056	5/2 1/2 - [521]				37	56	35		66	3
1072	7/2 7/2 - [514]	17	17	12	47	79	52	16	91	3
1128	9/2 5/2 - [512]	1	3	3	4	14	15	2.8	18	h
1154		467	292	142	11	16	10	275	22	1
1219	9/2 7/2 - [514]	2	4	5	4	21	16	3	29	h
1233		31	28	19	1.4	4	1.8	25	5	3
1265	7/2 1/2 - [521]			1.0	~15	47	31		69	(3)
1281	11/2 5/2 - [512]				~3	~3	4		4	
~1314	9/2 1/2 - [521]				<2	5	5		8	
1339					~3	5	~3		7	
1342		29	15	14				14		(3)
~1375					7	11	9		19	3
1376		11	6	4				5		
1390	9/2 9/2 - [505]?	28	28	23				25		3,h
1397	11/2 7/2 - [514]				~3	9	7		15	h
1441						2.7	2.2		5	
1443		11	11	5				9		(1)
1468					~5	~2	1.2		~3	
1476		268	263	126	7	13	6	232	24	1,3

(continued)

TABLE 3 (continued).

Energy keV	Assignment $IK^\pi[Nn_zA]$	Experimental cross section						Q-reduced cross section		In- ferred l -value
		(d,p) $\mu\text{b}/\text{sr}$			(d,t) $\mu\text{b}/\text{sr}$			(d,p) $\mu\text{b}/\text{sr}$	(d,t) $\mu\text{b}/\text{sr}$	
		60°	90°	125°	60°	90°	125°	90°	90°	
1489		37	20	21	2.2		2.3	17		
1514		<2	<2	~5				~2		
1550	13/2+, N = 6				7	13	13		26	6†
1558		190	150	67				124		1
1562	9/2+, N = 6				11	21	23		43	3,h
1583		19	25	19				21		3,h
1592					19	32	21		67	3
1631		131	100	50				81		1
1650					<4	9	7		20	
~1651		25	20	10				16		1
1679					4	8	7		19	3
1687		73	71	43				56		3
1692					4	8	3		18	
1711	13/2+, N = 6				3	7	11		17	6†
1723		87	107	75				83		3
1737					6	7	5		17	1
1740		87	62	35				48		1
1763					7	12	11		30	3
1790		118	67	36				52		1
1792					~3	7	5		19	
1816		119	138	118				104		3,h
1822					7	16	8		43	3
1827		260	130	77				99		1
1847		328	173	115				130		1
1950		129	117	93				86		3
1967					1.9	5	5		17	3,h
1969		63	52	<48				38		1
1989		49	37	<37				27		1
1989					3	7	4		24	
2014		88	56	42				40		1,3
2016					9	15	11		~54	3,1
2050		31	28	23				20		3
2068		74	55	32				38		1
2097		39	28	18				19		3
2137						~15	10		~54	
2134		110	68	41				46		1
2216						~12	5		~42	

* Energy from γ -ray measurements.† $l = 6$ from ($^3\text{He},\alpha$) data.

TABLE 4. Levels populated in ^{185}W .

Energy keV	Assignment $IK^\pi[Nn_zA]$	Experimental cross section						Q-reduced cross section		In- ferred l-value
		(d,p) $\mu\text{b}/\text{sr}$			(d,t) $\mu\text{b}/\text{sr}$			(d,p) $\mu\text{b}/\text{sr}$	(d,t) $\mu\text{b}/\text{sr}$	
		60°	90°	125°	60°	90°	125°	90°	90°	
0	3/2 3/2 - [512]	17	4	~2	3	<1	<1	5	<1	
24*	1/2 1/2 - [510]	~1.6	3	~3	5	5	3	4	2.7	
66*	5/2 3/2 - [512]	287	257	90	415	409	221	301	207	3
94*	3/2 1/2 - [510]	445	307	88	707	597	275	357	308	1
174*	7/2 3/2 - [512]	10	~10	1.3	3	2.4	1.5	~11	1.3	
188*	5/2 1/2 - [510]	<3	~4	0.6	14	19	9	~4	11	3
244*	7/2 7/2 - [503]	243	287	97	209	278	160	316	154	3
302	9/2 3/2 - [512]	12	10	6	7	19	19	11	11	h
334	7/2 1/2 - [510]	97	98	39	121	170	105	104	99	3
384	13/2 11/2 + [615]	15	28	17	17	53	46	30	32	6†
391*	9/2 7/2 - [503]						~5		~3	
~478	11/2 3/2 - [512]						~0.5		~0.4	
~492	9/2 1/2 - [510]					~1	~1.0		~0.8	
~570	11/2 7/2 - [503]			1.2		2.1	4	~5	1.4	h
666		100	56	17	16	16	10	54	11	1
706	11/2 1/2 - [510]	~8	5	2.8	~2	5	7	5	4	h,3
716	9/2 9/2 + [624]		3		11	19	13	3	15	3,h
733		156	101	28	48	59	33	95	45	1(3)
~789	9/2 9/2 - [505]	25	27	18	4	12	8	25	10	h,3
~801		29	34	8	1.1	1.6	1.3	31	1.3	
833		13	11	1.5	1.1	1.6	1.6	10	1.3	(1)
888	5/2 5/2 - [512]	<2	<3	~0.7	17	16	12	<3	14	3
904		<5	<2	4	3	10	4	<2	9	
921					2.7	5	3		5	3
986	7/2 5/2 - [512]	33	33	13	135	222	158	32	206	3
1008	1/2 1/2 - [521]						~170			
1013	1/2 - (3/2 - [512], γ)	106	73	26	334	485	~77	62	386	1
1020	13/2 9/2 + [624]					~23	18		~19	6†
1040	3/2 - (3/2 - [512], γ)	27	23	4	68	83	26	20	80	1
1058*	7/2 7/2 - [514]	~18	17	7	44	81	60	15	80	3
1073	5/2 - (3/2 - [512], γ)				9	17	7		17	3,1
1106	3/2 1/2 - [521]				31	42	21		43	1,3
1107		~35	~44	~6				~37		1,3
1118	5/2 1/2 - [521]				26	39	25		40	3
1120	9/2 5/2 - [512]							81		3,1

(continued)

TABLE 4 (continued).

Energy keV	Assignment $IK^\pi[Nn_zA]$	Experimental cross section						Q-reduced cross section		In- ferred l-value
		(d,p) $\mu\text{b}/\text{sr}$			(d,t) $\mu\text{b}/\text{sr}$			(d,p) $\mu\text{b}/\text{sr}$	(d,t) $\mu\text{b}/\text{sr}$	
		60°	90°	125°	60°	90°	125°	90°	90°	
1149		96	74	21				65		1
1154	7/2 - (3/2 - [512], γ)				22	30	20		28	3,1
1185		433	284	86		<3		229	<3	1
~1219	9/2 7/2 - [514]				~5	17	12		19	(h)
1222		437	315	91	~5	~10	5	251	~11	1
~1279		24	~26	~10				22		(3)
1290		244	197	63	10	18	9	154	21	1
1317					5	14	8		17	
1317		65	74	31				57		3
1335	7/2 1/2 - [521]				11	obsc	19		~25	
1343		19	23	10				17		3
1346					5	obsc	4			
1361	9/2 1/2 - [521]				2.3	~9	2		~11	
1382					6	12	6		15	1,3
~1402					7	28	23		37	h,3
~1410					4	~3	~2		4	
1428		111	66	19	3	7	4	49	9	1
1445		49	43	22				32		(3)
1448					23	34	20		48	3,1
1501		~36	21	8				15		1,3
1503					16	36	19		54	3,1
1542		1074	~570	181	9	14	10	~391	22	1
1561	13/2+, N = 6				11	32	26		51	
1561		284	254	140				183		(3)
1603		12	19	4				13		
1623		29	31	7				22		3,h
1627					4	7	4		9	6†
1646					<2	<5	4		<8	
1663		50	38	18				26		1,3
1666	9/2+, N = 6				19	25	19		44	1,3
1677		76	85	~22				58		3
~1683					~4	~5	6		~9	
1699		24	40	12				27		
1701					5	10	7		18	3
1722		28	~26	5				~18		1
1728					9	13	9		25	1,3

(continued)

TABLE 4 (continued).

Energy keV	Assignment $IK^\pi[Nn_zA]$	Experimental cross section						Q-reduced cross section		In- ferred l-value
		(d,p) $\mu b/sr$			(d,t) $\mu b/sr$			(d,p) $\mu b/sr$	(d,t) $\mu b/sr$	
		60°	90°	125°	60°	90°	125°	90°	90°	
1745		63	48	15				32		1
1800		42	33	9				22		1
~1830		~72	~39	~11				~25		1
1845		~105	~24	~31				~22		
1846	13/2+, N = 6				4	~30	24		~64	6†
1860					7	~24	11		~52	
1874					4	~5	5		~11	
1886		~36	33	9				21		1
1904		16	19	<4				12		
1915					7	16	7		38	
1937					6	13	11		30	3
1952					8	22	14		~53	3,1
1959		83	~41	25				~26		
1986					9	11	~9		28	1
2031		~88	~61	~18				~38		1
~2038					~7	~8	9		~20	

* Energy from γ -ray measurements.

† l = 6 from ($^3\text{He},\alpha$) data.

84 and 20 mb/sr at 60°, 90° and 125°, respectively. These values are in reasonable agreement with a recent measurement¹⁸.

Cross sections were determined from the total number of tracks in the peaks. The high level densities often required the use of an unfolding procedure which was based on the experimental peak shape in each spectrum. Estimated uncertainties on absolute cross sections greater than 20 $\mu b/sr$ are about $\pm 20\%$ while for smaller cross sections they might be as high as $\pm 50\%$, especially at 60°. Relative cross sections of well resolved peaks within each spectrum are estimated to be accurate within $\pm 10\%$. The excitation energies were determined from the peak centroids as a weighted average of the results at all three angles and, where possible, of both deuteron induced reactions. Where energies are already known, the agreement is generally very close. We assign errors of ± 6 keV per MeV of excitation to well resolved peaks with 90° cross section of 20 $\mu b/sr$ or more.

TABLE 5. Levels populated in ^{187}W .

Energy keV	Assignment $IK^\pi [Nn_z A]$	Experimental cross section			Q-reduced cross section	Inferred l-value
		(d,p) $\mu\text{b/sr}$			(d,p) $\mu\text{b/sr}$	
		60°	90°	125°	90°	
0	3/2 3/2 - [512]	69	34	14	37	1
77*	5/2 3/2 - [512]	231	201	108	213	3
205*	3/2 1/2 - [510]	437	268	126	272	1
303*	5/2 1/2 - [510]	30	21	14	21	3
329	9/2 3/2 - [512]	< 2	~ 5	10	~ 5	<i>h</i>
351	7/2 7/2 - [503]	278	219	137	211	3
366	13/2 11/2 + [615] ^a	< 9	< 35	~ 29	~ 34	<i>h</i>
432*	7/2 1/2 - [510]	77	75	48	71	3
598	9/2 9/2 - [505] ^a	16	26	26	23	<i>h</i>
641*	5/2 5/2 - [503]?	122	103	60	90	3
~ 731		3	~ 5	4	~ 4	
782*		535	310	145	260	1
816*		641	406	195	336	1
853		207	125	63	102	1
866*		~ 50	~ 62	~ 25	~ 50	(3)
892*		54	41	20	33	1,3
961		30	27	20	21	3
980		78	56	32	44	1,3
998		~ 6	~ 9	3	~ 7	
1034		8	7	4	5	
1072		54	53	36	40	3
1087		~ 21	20	11	15	3
1114		~ 7	13	9	10	(<i>h</i>)
1139		30	19	8	14	1
1196			15		11	
1234		70	52	~ 45	37	3
1267		15	19	~ 26	14	<i>h</i>
1313		456	242	112	170	1
1349		218	170	73	118	1
1361		123	121	75	84	3
1384		293	186	101	127	1
1416		135	84	~ 58	57	3,1
1426		202	245	~ 121	166	
1479		40	45	23	30	3,1
1494		25	11	4	8	1
1537		583	332	156	217	1
1566		~ 55	53	24	35	1,3

(continued)

TABLE 5 (continued).

Energy keV	Assignment $IK^\pi [Nn_zA]$	Experimental cross section			Q -reduced cross section	Inferred l -value
		(d,p) $\mu\text{b}/\text{sr}$			(d,p) $\mu\text{b}/\text{sr}$	
		60°	90°	125°	90°	
1591		296	167	85	107	1
1602		~ 99	79	~ 33	51	(1)
1633		~ 24	18	17	11	(3)
1673		29	~ 11	6	~ 7	1
1691		~ 11	14	7	9	
1719		99	118	54	73	
1749		41	48	22	30	
1771		46	~ 21	14	~ 13	
1825		108	59	37	35	1(3)
1844		~ 43	20	11	12	1
~ 1907		obsc	~ 88	48	~ 51	
~ 1917		obsc	~ 50	~ 23	~ 29	
~ 1941		obsc	~ 60	29	~ 34	
~ 2017		obsc	~ 60	35	~ 34	

* Energy from γ -ray measurements.

^a The assignments of these two levels could be reversed (cf. sect. 4.7).

The (d,p) cross sections at 60° for ^{182}W , ^{184}W and ^{186}W targets were determined earlier¹²⁾ by similar techniques with accuracies comparable to those assigned here. For ^{187}W , the two sets of results agree fairly well. However, the deviations for ^{183}W and ^{185}W , on the average, are more nearly a factor of 1.3 to 1.8.

3.4. Q -Reduction and DWBA Calculations

It is necessary to consider the Q -dependence of the transfer reactions when comparing theoretical cross section predictions to experimental results. Since initially most of the Nilsson assignments and hence the Q -values for the transfer into these orbitals are not known, it is convenient to calculate all theoretical cross sections at standard Q -values, namely, +3.0 MeV for the (d,p) reaction, and -2.0 MeV for the (d,t) reaction. All experimental cross sections are reduced to these standard Q -values by means of the theoretical Q -dependence calculated from the DWBA. The theoretical Q -dependence is quite similar for the different l transfers (fig. 15) and there-

TABLE 6. Optical model parameters for the DWBA calculations.

Particle	V (MeV)	W (MeV)	r_0 (f)	a (f)	r'_0 (f)	a' (f)	r_C (f)
Proton.....	55.0	17.5	1.25	0.65	1.25	0.47	1.25
Deuteron	104.5	17.3	1.15	0.81	1.34	0.68	1.15
Triton	154.0	12.0	1.10	0.75	1.40	0.65	1.25
Bound State							
Neutron	^a	—	1.25	0.65	—	—	—

^a Searched on to fit empirical binding energies.

TABLE 7. Differential single particle transfer cross sections calculated from the DWBA.

($\theta = 90^\circ$; $Q(d,t) = -2$ MeV; $Q(d,p) = 3$ MeV).

l	$\varphi_l(d,t)$ $\mu b/sr$	$\varphi_l(d,p)$ $\mu b/sr$
0	870	923
1	567	585
2	489	531
3	203	228
4	133	164
5	27	34
6	12	17

fore an average Q -dependence could be used. The latter is also shown, for each angle and reaction, in fig. 15. This gives rise to two sets of cross sections, the actual measured ones and a set of Q -reduced cross sections that, according to the DWBA, would have occurred if each transition had had the standard Q -value. Whenever cross section values are discussed below, unless otherwise noted, they refer to the Q -reduced differential cross sections at 90° .

The optical potential parameters used (see table 6) are those calculated for a spherical target nucleus of mass and charge 183 and 74 from the standard¹⁹⁻²⁰⁾ prescriptions. In agreement with the results of SIEMSSSEN and ERSKINE¹⁴⁾ who made more extensive (d,p) angular distribution measurements, this has been found to be a better procedure than to use parameters obtained by fitting the deuteron elastic scattering cross section data. A recent (t,d) investigation²¹⁾ suggests the superiority of this procedure for the (d,t) reaction as well.

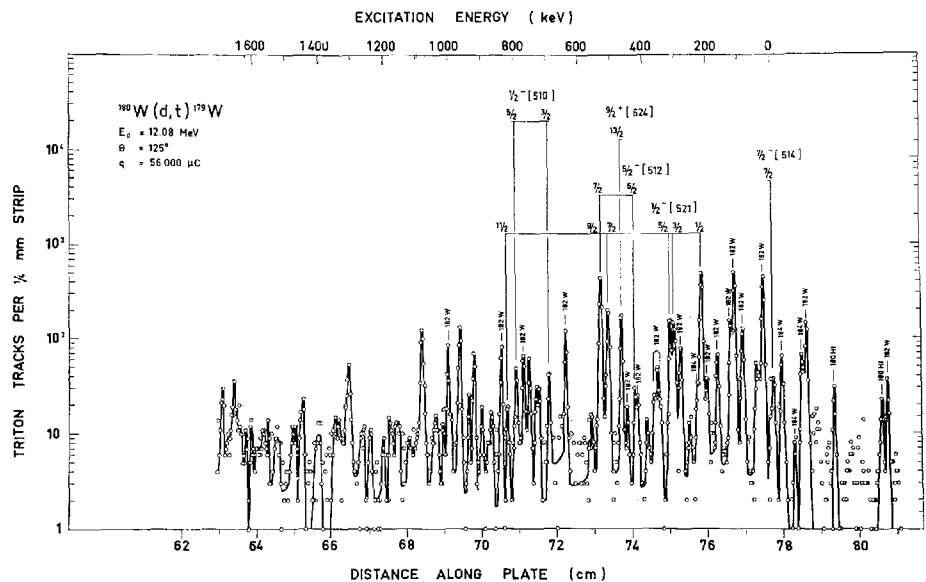


Fig. 1. Triton spectrum for the reaction $^{180}\text{W}(d,t)^{179}\text{W}$ at 125° .

It should finally be noted that the DWBA calculations give strong diffraction patterns for low even l transfers and at high Q -values, which sensitively depend on slight changes of the optical model parameters and probably are not physical. An arbitrary but consistent smoothing procedure³⁾ was applied to the calculated angular distributions prior to the extraction of the single-particle transfer cross sections used for calculation of the theoretical fingerprint patterns. The resulting (normalized) single-particle transfer cross sections are given in table 7.

3.5. Cross Section Angular Distributions and l values

Since the angular distributions are relatively structureless at this low bombarding energy, the cross section ratios from the three angles of measurement, 60° , 90° and 125° , provided an important guide in estimating the transferred l -values. For the states of previously known spin and parity, it has been found that the three experimental reduced cross section ratios $\sigma(60^\circ)/\sigma(90^\circ)$, $\sigma(125^\circ)/\sigma(90^\circ)$ and $\sigma(125^\circ)/\sigma(60^\circ)$ fall into separate classes corresponding to $l = 1$, 3 and ≥ 5 transfers (fig. 16). For example, in the (d,t) reaction, the ratio $\sigma(125^\circ)/\sigma(90^\circ)$ for $l = 1$, 3 and ≥ 5 transfers ex-

TABLE 8. Q -values and neutron separation energies for W nuclei.

Mass A	$Q(d,t)$ $A \rightarrow A-1$ keV	$Q(d,p)$ $A-1 \rightarrow A$ keV	$S_n(d,t)$ keV	$S_n(d,p)$ keV	S_n from mass tables ²²⁾ keV
180	-2155 ± 15		8413 ± 15		
181		4468 ± 15		6693 ± 15	6947 ± 36
182	-1809 ± 10		8067 ± 10		7987 ± 22
183	57 ± 15	3979 ± 10	6201 ± 15	6204 ± 10	6187 ± 3
184	-1154 ± 10	5187 ± 15	7412 ± 10	7412 ± 15	7418 ± 19
185		3533 ± 10		5758 ± 10	5748 ± 5
186	-939 ± 10		7197 ± 10		7213 ± 43
187		3240 ± 10		5465 ± 10	5460 ± 5

hibits values in the ranges 0.5–0.8, 0.8–1.5 and 3.0–6.0 respectively. For the few transitions known to involve $l = 4$ transfer, this ratio is somewhat higher than the average value which has been observed for $l = 3$ transfers. However, with the limited angular distribution data available it was generally not possible to distinguish reliably between adjacent l -values.

For states of previously unknown spin and parity, l transfer values have been inferred from the experimental angular distributions only when all three cross section ratios indicate the same angular momentum transfer. In some other cases, where the experimental data are less clearcut, no unique l has been assigned although preferences are indicated. The angular distributions for all states which are populated with moderate to strong intensity in the (d,p) and (d,t) reactions on ^{186}W are displayed in fig. 17, which illustrates the classification of the observed transitions into three distinct categories. The inferred l -values for all the nuclei studied are indicated in tables 1 to 5. The symbol “ h ” is used for $l \geq 5$.

The aforementioned uncertainty of ± 1 unit of angular momentum in the inferred l -values was not a very serious limitation for the hole states since no even parity orbitals with strong population cross sections of low l -transfer are expected for the wolfram nuclei; the important even parity states are those originating from the $i_{13/2}$ spherical state which are populated predominantly with $l = 6$ transfer and which have, in any case, been identified by the $(^3He, \alpha)$ reaction studies. On the other hand, our inability to use the angular distribution data for parity assignment was a definite drawback in interpreting the (d,p) spectra.

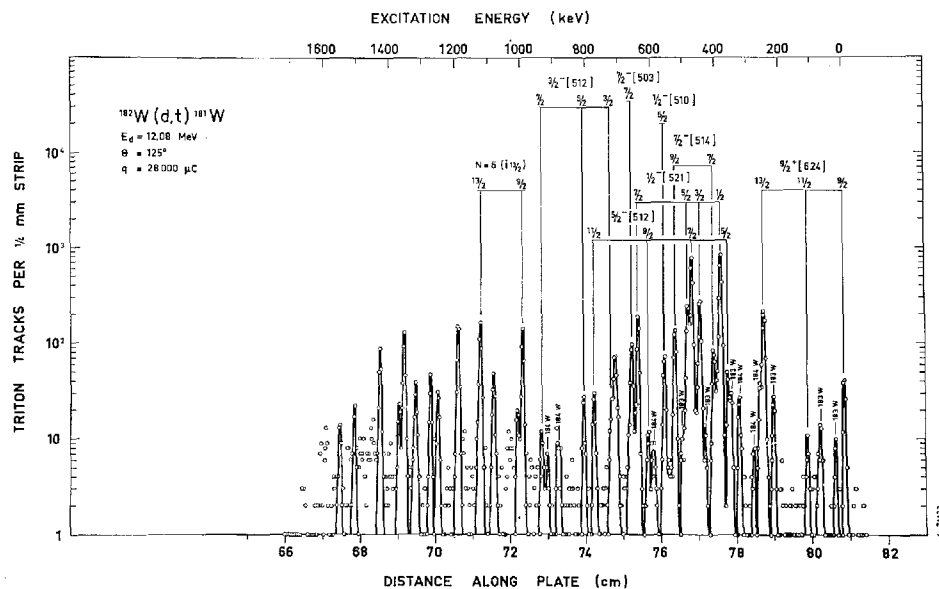


Fig. 2. Triton spectrum for the reaction $^{182}\text{W}(d,t)^{181}\text{W}$ at 125° .

3.6. Ground State Q Values

In all spectra the ground state or a low-lying state of known excitation energy is well populated and hence the Q -values can be accurately determined. These results are listed in table 8, together with the neutron separation energies S_n calculated from the relations

$$S_n(A) = 6.258 \text{ MeV} - Q_{(dt)} (A \rightarrow A - 1)$$

and

$$S_n(A) = 2.225 \text{ MeV} + Q_{(dp)} (A - 1 \rightarrow A)$$

Also included are the results obtained from the reactions with a ^{183}W target. The agreement with the 1964 mass tables²²⁾ is fairly good except for the ^{181}W neutron separation energy for which the present result is about 250 keV lower than the earlier value. The mass of ^{179}W was not previously known.

4. Nilsson Assignments

The energy level systematics of well studied neighbouring nuclei provided a starting point for the interpretation of the observed level spectra as they indicated which orbitals were likely to occur as low energy excitations in

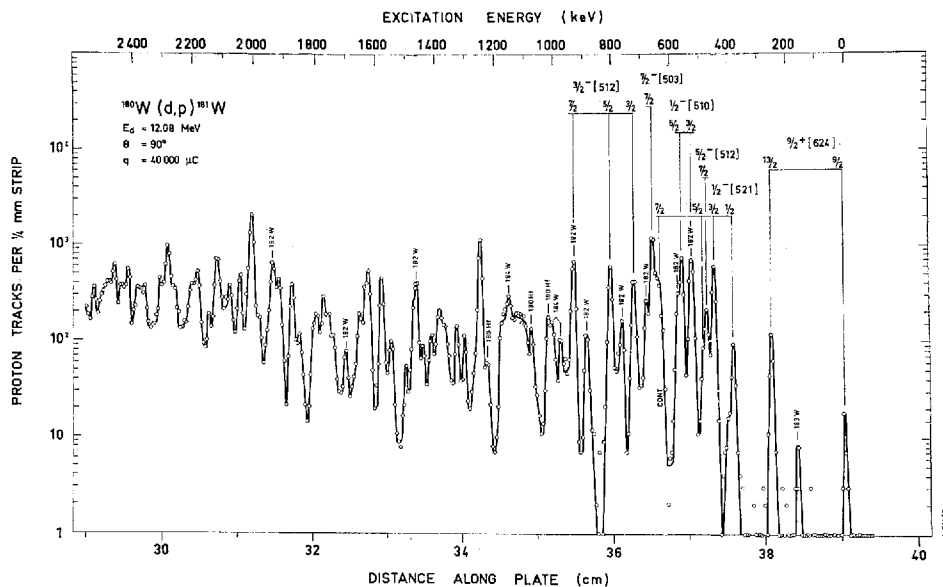


Fig. 3. Proton spectrum for the reaction $^{180}\text{W}(d,p)^{181}\text{W}$ at 90° .

the wolfram nuclei. For each expected orbital a search was made for the corresponding band which was required to have reasonable rotational spacings and to exhibit absolute cross sections and a fingerprint pattern resembling those calculated from the DWBA and the Nilsson model. In this search the spin restrictions implied by the inferred l -values and the observed ratios of (d,p) to (d,t) cross-sections were also kept in mind. Several straightforward identifications resulted. For example, the $1/2 - [521]$ and $5/2 - [512]$ bands appeared in all the (d,t) spectra with fingerprint patterns closely resembling those expected (figs. 18 a and b). For some other bands, e.g. the $7/2 - [514]$ band, only tentative identifications were possible at first as the observed cross sections bore little resemblance to the predicted fingerprint patterns (fig. 18 c). In many cases subsequent Coriolis coupling calculations explained the apparent deviations from theory satisfactorily and solidified the assignments. The striking effects which can arise from strongly coupled bands are illustrated in fig. 19 where the observed cross sections for the close lying $1/2 - [510]$ and $3/2 - [512]$ bands, which were identified in all the (d,p) spectra, are compared with the fingerprint patterns calculated with no mixing included.

The assignments made are listed in tables 1 to 5 and in the level schemes

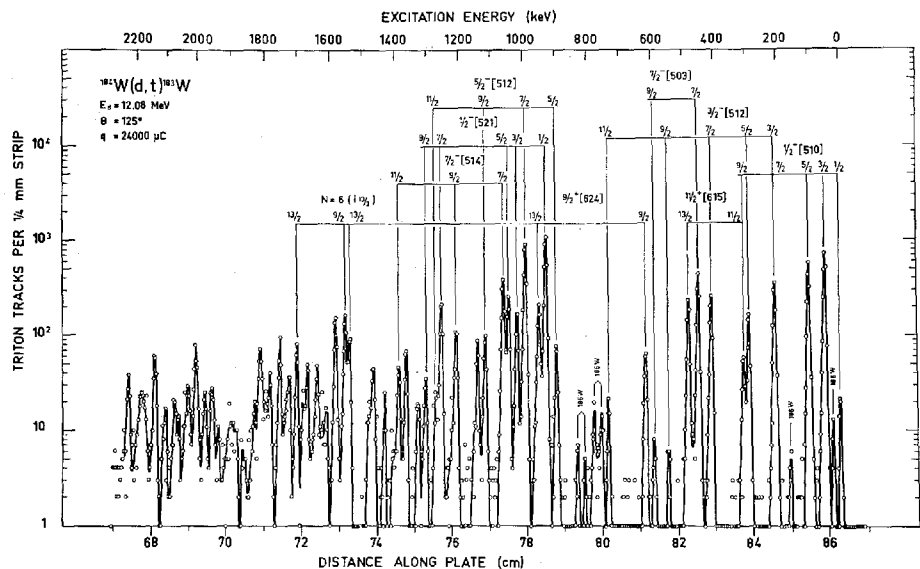


Fig. 4. Triton spectrum for the reaction $^{184}\text{W}(d,t)^{183}\text{W}$ at 125° .

of figs. 10 to 14. All supporting arguments will not be discussed for each assignment since these are often similar and similar also to those used in previous studies. Detailed comments on the assignments and on the Coriolis mixing calculations are given in later sections.

In the (d,t) spectra essentially all states up to about 1400 keV excitation energy were assigned along with a few tentative even parity assignments at higher excitation energies. The experimental data for the higher lying states are however of poorer quality since the (d,t) cross sections are smaller for the more negative Q -values (fig. 15).

At the deformation of the wolfram nuclei the Nilsson model predicts a distinct energy gap above the neutron number 118. In the (d,p) spectra essentially all Nilsson orbitals below this gap were identified at excitation energies below 700 keV. The spectra clearly exhibit a reduced level density in the energy region above these states. The orbitals expected at higher excitation energies could, however, not be localized individually due to the complexity of the spectra (sect. 4.9).

The detailed discussion below therefore is limited to the negative parity Nilsson orbitals $7/2 - [514]$, $5/2 - [512]$ and $1/2 - [521]$, which occur as hole excitations, the $1/2 - [510]$ and $3/2 - [512]$ orbitals near the Fermi surface and the $7/2 - [503]$ and $9/2 - [505]$ orbitals which are particle excitations in

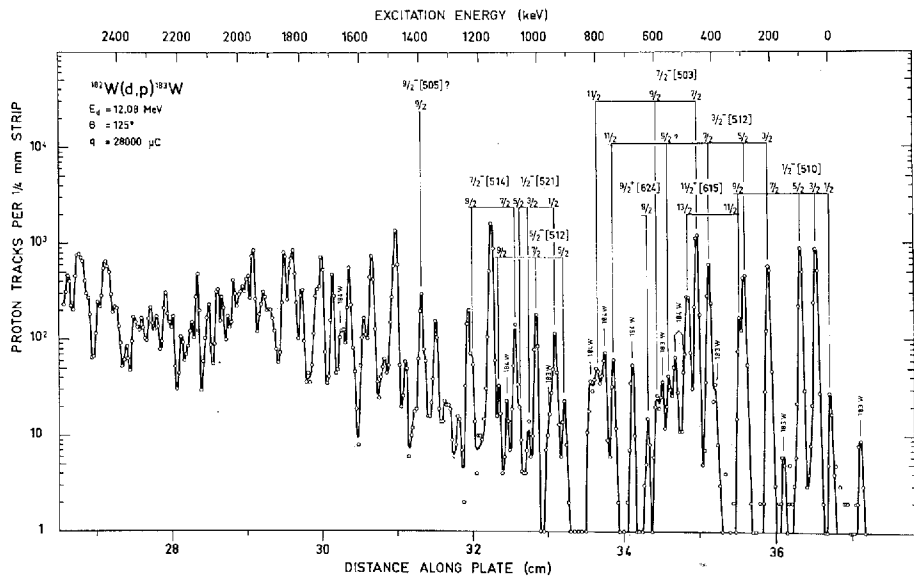


Fig. 5. Proton spectrum for the reaction $^{182}\text{W}(d,p)^{183}\text{W}$ at 125° .

the wolfram nuclei. In addition, the strongly mixed $i_{13/2}$ even parity orbitals $11/2 + [615]$, $9/2 + [624]$, $7/2 + [633]$, $5/2 + [642]$, $3/2 + [651]$ and $1/2 + [660]$ are discussed together in a single section. These orbitals span an energy interval of about 4.5 MeV of the Nilsson diagram, and no other orbitals are expected in this energy region.

The energy levels in ^{179}W were populated only through the (d,t) reaction. Most of the observed states up to 900 keV of excitation have been assigned. These assignments are in general agreement with the results of a recent ^{179}Re decay study²³⁾.

The analysis of the reaction data for ^{181}W was greatly aided by a parallel study of the ^{181}Re decay²⁴⁾. In ^{181}W , the strongly mixed $1/2 - [510]$ and $1/2 - [521]$ bands occur close together but on opposite sides of the Fermi surface, thus giving rise to rather unusual mixing effects. Although it has been possible to account satisfactorily for many of the observed effects with a Coriolis treatment, some anomalies remain (see section 5.4), and in general the population cross sections and level energies in ^{181}W are not as well understood as in the other nuclei. In the (d,t) spectrum, most groups up to 1200 keV have been assigned, and in the (d,p) spectrum, all those groups which could definitely be attributed to ^{181}W . Due to the presence of other W isotopes in the ^{180}W target, the (d,p) spectrum was particularly complex. The analysis

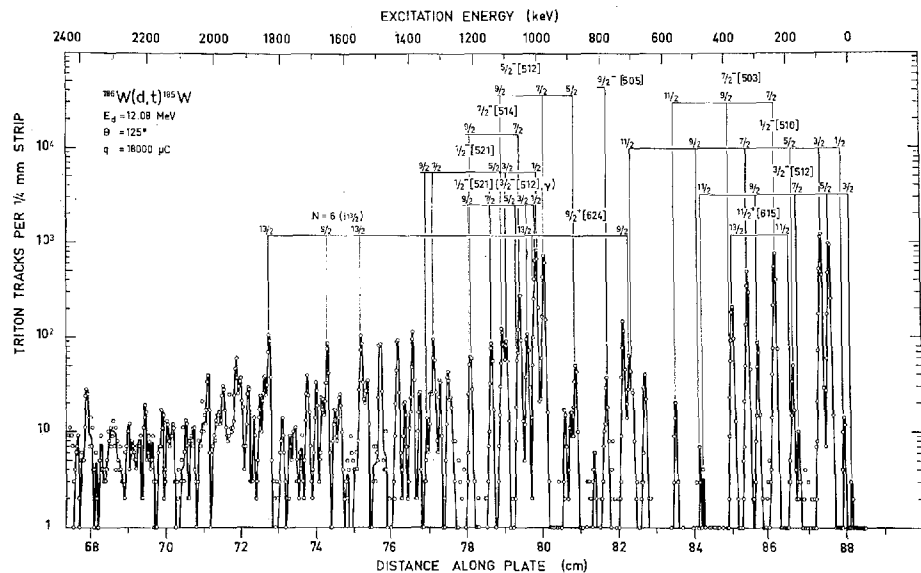


Fig. 6. Triton spectrum for the reaction $^{186}\text{W}(d,t)^{185}\text{W}$ at 125° .

was therefore limited to states below 1200 keV, and the (d,p) cross sections into ^{181}W are less accurately determined.

Extensive level schemes for ^{183}W and ^{185}W were established using both the (d,p) and (d,t) reactions. All the observed hole states up to 1400 keV have been interpreted, but the high excitation energy portions of the (d,p) spectra are not well understood. The low lying levels of ^{183}W and ^{185}W were previously investigated in numerous radioactive decay studies, and the reaction data fully confirm the conclusions reached in the more recent investigations²⁵⁻²⁷).

All energy levels below 600 keV populated in ^{187}W by the (d,p) reaction have been assigned. Our results are in good agreement with those of ERSKINE's earlier reaction study¹²⁾ although two additional high K orbitals have been located in the present work.

4.1. The $7/2$ -[514] Orbital

In ^{179}W , the $7/2$ -[514] orbital forms the ground state. Only the $7/2$ -state of the band could be observed in the (d,t) spectra because of target contamination.

In ^{181}W , the $7/2$ -[514] band head was previously known²⁸⁾. In addition, the $9/2$ -member of the band has been identified in the (d,t) spectra.

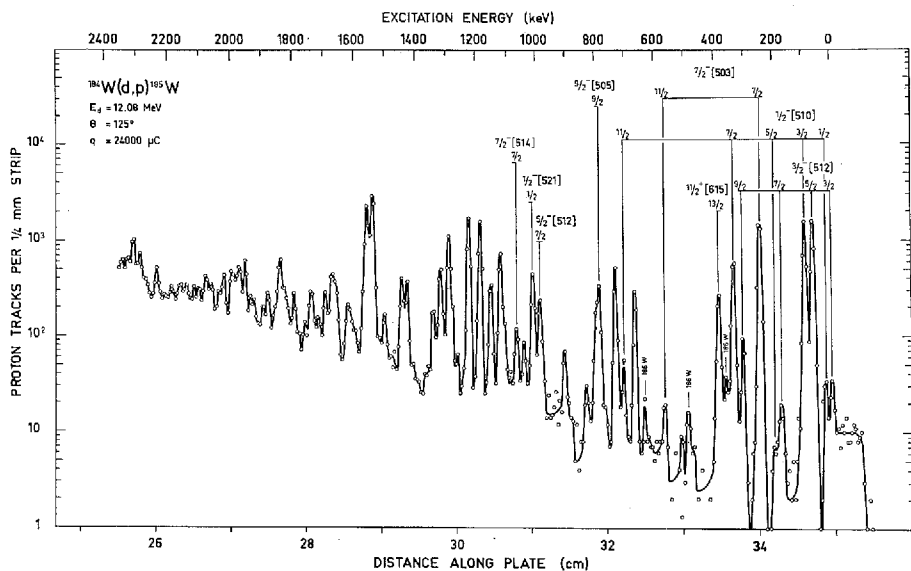


Fig. 7. Proton spectrum for the reaction $^{184}\text{W}(d,p)^{185}\text{W}$ at 125° .

In ^{183}W and ^{185}W , the band has been identified at approximately 1 MeV of excitation. It has not been observed in ^{187}W which could be populated by the (d,p) reaction only.

The observed fingerprint patterns are quite different from the predicted one which has equally populated $7/2$ and $9/2$ states (fig. 18 c). The sharp variations in population cross sections for the $7/2$ state are ascribed to coupling with the close-lying strong $7/2\ 5/2 - [512]$ state, as will be discussed in sect. 5.

4.2. The $1/2 - [521]$ Orbital

The $1/2 - [521]$ band is easily identified because of the strongly populated $1/2$ and the comparatively strong $3/2$, $5/2$ and $7/2$ band members. Furthermore, the band has a characteristic decoupling parameter of about 0.8.

In ^{179}W the band was already known²³⁾ and is confirmed by the reaction data.

In ^{181}W the $1/2 - [521]$ band head is found at 385 keV, and the higher band members up to $I = 7/2$ can clearly be identified. However, the observed decoupling parameter of $a = 0.48$ is significantly smaller than found in the

other wolfram nuclei. This definite assignment conflicts with the previous suggestion²⁸⁾ of $1/2\ 1/2 - [510]$ for the 385 keV state.

In ^{183}W the band is easily identified with the band head at 936 keV.

In ^{185}W the assignment is also rather straightforward with the band head at 1008 keV, but a significant reduction of the total intensity (fig. 18 a) compared to ^{183}W is obvious. However, in ^{185}W several groups around 1 MeV have energy spacings and l -values which together are suggestive of an additional $K = 1/2$ band. It is tentatively proposed that the $1/2 - [521]$ strength in ^{185}W is split, and that approximately one third of it contributes to a $K=2$ gamma vibration at 1013 keV based on the $3/2 - [512]$ ground state. The smaller decoupling parameter ($a = 0.2$) of this latter tentative $K = 1/2$ band supports this interpretation.

In ^{187}W the band is too far below the Fermi surface to be populated in the (d,p) reaction.

4.3. The $5/2 - [512]$ Orbital

This orbital is characterized by the large population of the $7/2 -$ rotational member.

In ^{179}W and ^{181}W the band was already known^{23, 28)} and it has been confirmed by the (d,t) data. In ^{181}W , the $9/2 -$ and $11/2 -$ band members have also been located in the present work.

In ^{183}W and ^{185}W the band is identified around 900 keV and has in both cases been definitely localized.

The band has not been seen in ^{187}W .

It is consistently observed that the $5/2$ member is populated with a cross section 50 to 100 times larger than the $0.2\ \mu\text{b}/\text{sr}$ predicted by the Nilsson model. A similar enhancement was earlier found in the rare earth region for this state.

4.4. The $1/2 - [510]$ Orbital

The $1/2 - [510]$ band is expected to be characterized by a very strong $3/2 -$ group and a moderately strong $5/2 -$ group. In the wolfram nuclei, this band is strongly perturbed by the near-lying $3/2 - [512]$ band (fig. 19 a).

In ^{179}W a tentative identification of the band head has been made at ~ 627 keV. A previous assignment²³⁾ at 704.9 keV leading to $3/2$ and $5/2$ states at 768.7 and 806.9 keV is not consistent with the present data which show no peaks at these energies in contrast to expected cross sections of $10 - 20\ \mu\text{l}/\text{sr}$.

In ^{181}W the band head is placed at 457.7 keV. The identification of the

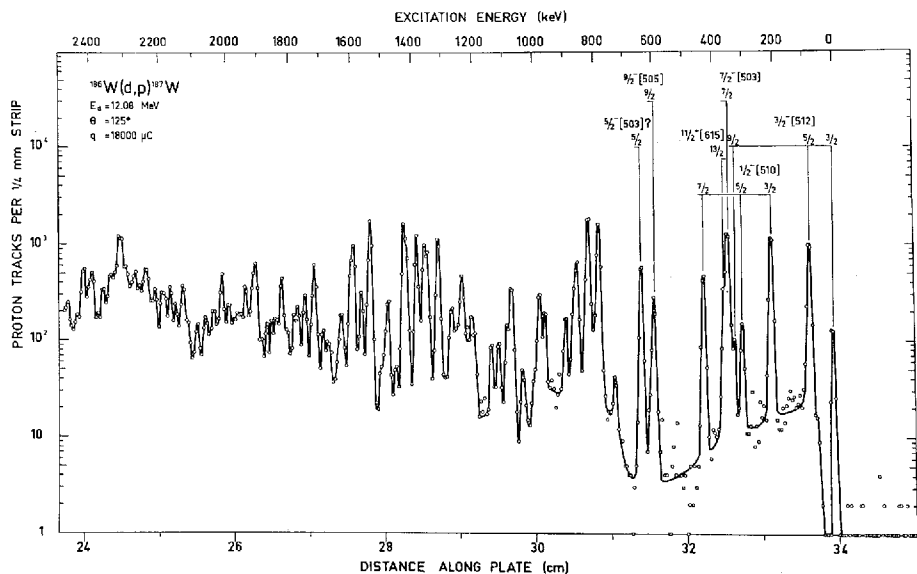


Fig. 8. Proton spectrum for the reaction $^{186}\text{W}(d,p)^{187}\text{W}$ at 125° .

band is based on the combined information from the present reaction data and the parallel investigation of the ^{181}Re decay²⁴). An earlier²⁸) assignment at 746 keV is incompatible with the reaction data as well as the more recent decay results.

In ^{183}W and ^{187}W the $1/2 - [510]$ orbital was previously known²⁸), and the assignments are confirmed by the present reaction data.

In ^{185}W , an earlier companion study²⁶) of ^{185m}W decay, which utilized some of the present reaction data, established the location of the $1/2 - [510]$ band as well as the $3/2 - [512]$ and $11/2 + [615]$ bands discussed below.

4.5. The $3/2 - [512]$ Orbital

This orbital is characterized by strong $3/2 -$ and $5/2 -$ groups, but in the W nuclei the band is strongly perturbed (fig. 19 b) by coupling to the $1/2 - [510]$ band discussed above.

In ^{179}W the band has not been observed, but it has been identified in ^{181}W where it was not previously known.

In ^{183}W the reaction data confirm the previously well established assignment. All rotational members up to $I = 9/2$ were clearly observed. A high l -group which is observed at 742 keV in both reactions is tentatively assigned as the $11/2 -$ rotational state.

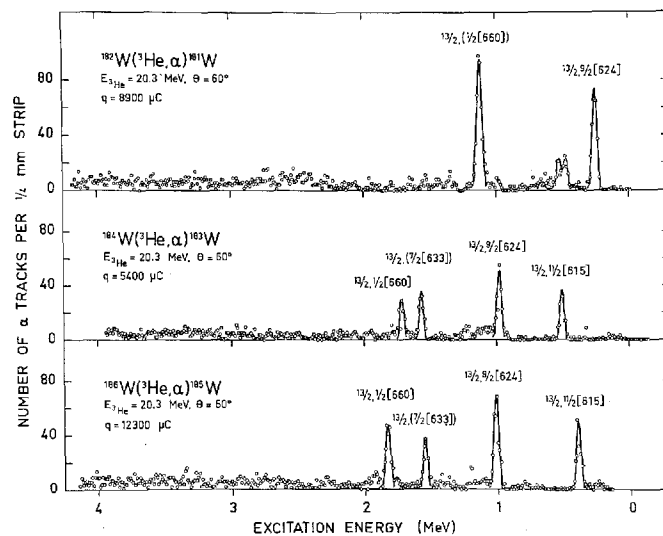


Fig. 9. Alpha-particle spectra for the reactions $^{182}\text{W}(^3\text{He},\alpha)^{181}\text{W}$, $^{184}\text{W}(^3\text{He},\alpha)^{183}\text{W}$ and $^{186}\text{W}(^3\text{He},\alpha)^{185}\text{W}$ at 60° .

In ^{185}W the band members up to $I = 7/2$ were located in the ^{185}mW decay study in agreement with the present reaction data. The latter also established the $9/2-$ and, tentatively, the $11/2-$ member.

In ^{187}W , the (d,p) spectrum clearly shows the $3/2-$, $5/2-$ and $9/2-$ members of the $3/2-[512]$ ground state band. Because of mixing, the cross section for the $7/2-$ state is expected to be small (cf. table 17 and fig. 28) and the state could not be observed because of a fairly high back-ground in this region of the spectrum. The calculated perturbed energy of 186.5 keV agrees with earlier (n,γ) results²⁹⁾, although such a state has not been observed in a more recent (n,γ) investigation³⁰⁾.

4.6. The $7/2-[503]$ Orbital

The $7/2-[503]$ orbital occurs as a particle excitation in the wolfram nuclei and is thus mainly observed in the (d,p) reaction. The Nilsson model predicts strong population for the $7/2-$ state only.

In ^{181}W a group at 662 keV is assigned to this orbital, in disagreement with a previous²⁸⁾ assignment (at 807.9 keV) but in accord with the recent decay study²⁴⁾.

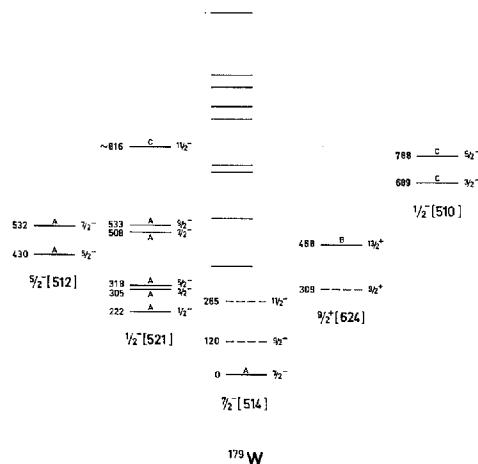


Fig. 10. Level scheme for ^{179}W . The letters A, B, C denote certain, probable and tentative assignments, respectively. Hole excitations are shown to the left, particle excitations to the right. Band members established in other studies but not observed in the transfer reactions are indicated by dashed lines. The unassigned levels in the energy region where assignments were made are shown above the ground band with their particle or hole character indicated.

The present results agree with earlier proposed assignments^{27, 28)} in ^{183}W , ^{185}W and ^{187}W , and some additional high spin band members have been identified.

It is worthy of note that the population cross sections for the $7/2\ 7/2 - [503]$ state in the (d,t) reactions were consistently 40–80 μb larger than the values calculated from the pairing factor (cf. tables 14–16 in the appendix). It is possible that this reflects an admixture of the $7/2\ 5/2 - [512]$ hole state which has a large C_{β} coefficient and is also coupled to the $7/2 - [503]$ orbital through a large matrix element, although our present treatment of Coriolis coupling and pairing does not predict (d,t) cross sections of the observed magnitude.

4.7. The $9/2 - [505]$ Orbital

The $9/2 - [505]$ orbital is difficult to place since only the $9/2$ state should be populated and by the (d,p) reaction only. However, in ^{189}Os and ^{191}Os the state occurs²⁸⁾ in the ground state region and it therefore is expected at moderate excitation energies in the wolfram nuclei.

In ^{183}W the lowest candidate for the $9/2 - [505]$ state is observed at 1390

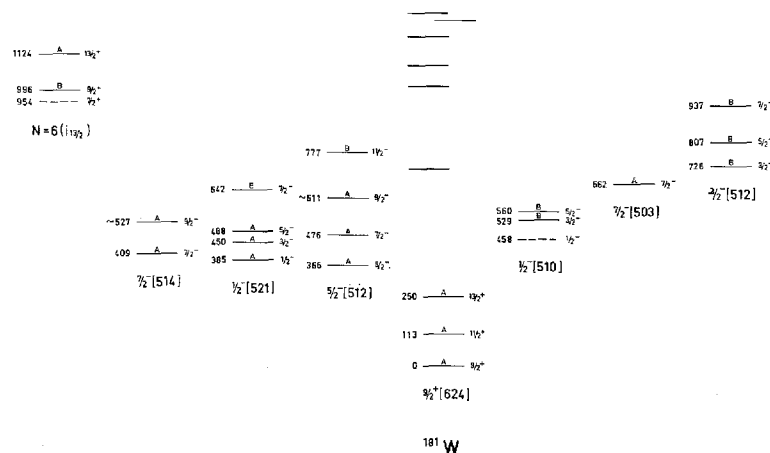


Fig. 11. Level scheme for ^{181}W . See caption to Fig. 10.

keV and is tentatively assigned as such although several higher lying levels (e.g. at 1582 keV) cannot be ruled out. The fact that the $13/2 + [606]$ and the $j_{15/2}$ Nilsson orbitals which have the same cross section characteristics might also occur in this energy region further complicates this assignment.

In ^{185}W the assignment at 789 keV is somewhat more definite. Below 1300 keV only the two states at 716 keV and 789 keV have approximately the expected cross section and an angular distribution showing high angular momentum transfer. Of these, the 789 keV is more strongly populated in the (d,p) reaction than in the (d,t) reaction and is therefore preferred for the $9/2 - [505]$ assignment. Furthermore, the 716 keV (d,t) group has an $l = 4$ type angular distribution and is most probably the $9/2 \ 9/2 + [624]$ level.

In ^{187}W , two groups with high angular momentum transfer are observed, at 366 keV and 598 keV. These two groups probably belong to the $9/2 \ 9/2 - [505]$ and the $13/2 \ 11/2 + [615]$ particle excitations, but it is difficult to distinguish between them since both states are expected to be populated with cross sections of 30 to 60 $\mu\text{b}/\text{sr}$. Energy systematics of the $11/2 + [615]$ orbital would suggest the lower state to be the $13/2 +$ state and it is shown as such in the figures although there are some problems with this choice of assignments. For example, with the $9/2 \ 9/2 - [505]$ state placed at 598 keV, a mixing calculation predicts that the $9/2 \ 9/2 - [505]$ and the $9/2 \ 7/2 - [503]$ states should receive comparable cross sections of 20 to 30 $\mu\text{b}/\text{sr}$. The (d,p) spectrum shows no indication of the latter state; its cross section is certainly

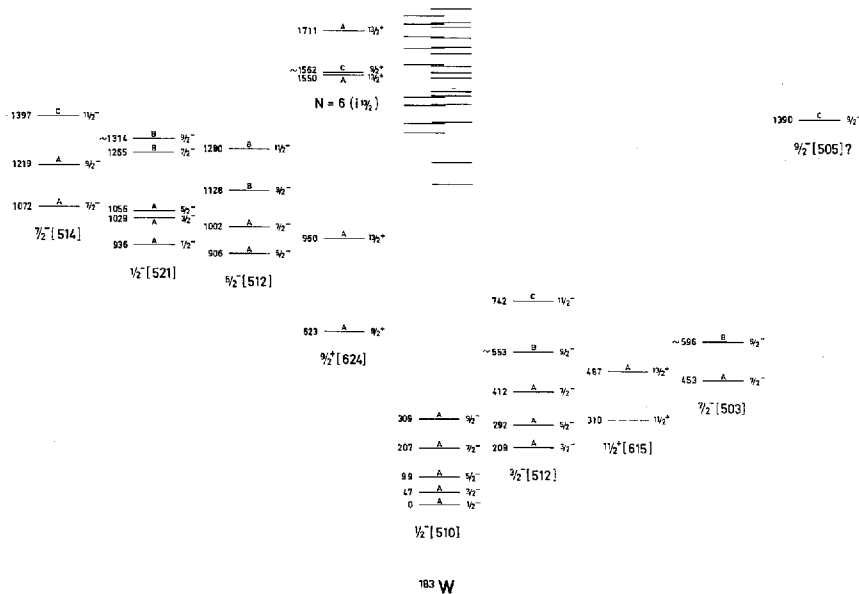


Fig. 12. Level scheme for ^{183}W . See caption to Fig. 10.

less than $5 \mu\text{b}/\text{sr}$. A further difficulty is our failure* to observe an isomeric state in ^{187}W , analogous to the 100 seconds $11/2 \ 11/2 + [615] E3$ isomer²⁶⁾ at 197.8 keV in ^{185}W . In summary, although the two observed high spin levels probably represent the $13/2 \ 11/2 + [615]$ and $9/2 \ 9/2 - [505]$ states, no clear choice between the alternative interpretations can be made here.

4.8. The $N = 6$ Orbitals from the $i_{13/2}$ Shell

For the seven $N = 6$ orbitals with $K = 1/2$ to $K = 13/2$ stemming from the $i_{13/2}$ spherical state only the $13/2 +$ rotational band members are predicted to be populated with appreciable cross sections. As mentioned before, these states are difficult to isolate by the (d,t) or by the (d,p) reaction alone. However, those lying below the Fermi surface are clearly identified¹¹⁾ by the combined information from the (d,t) and the $(^3\text{He},\alpha)$ reactions. In the wolfram nuclei the Fermi surface is situated close to the $11/2 + [615]$

* In the γ -spectrum recorded with a $\text{Ge}(\text{Li})$ counter immediately after thermal neutron activation of ^{186}W the expected isomer was not observed³²⁾. If one assumes a capture cross section ratio for the formation of the ground state and the isomeric state comparable to those found³³⁾ for this isomer in ^{183}W and ^{185}W the upper limit for the half life of the $11/2 + [615]$ isomer in ^{187}W is $T_{1/2} \leq 10$ seconds.

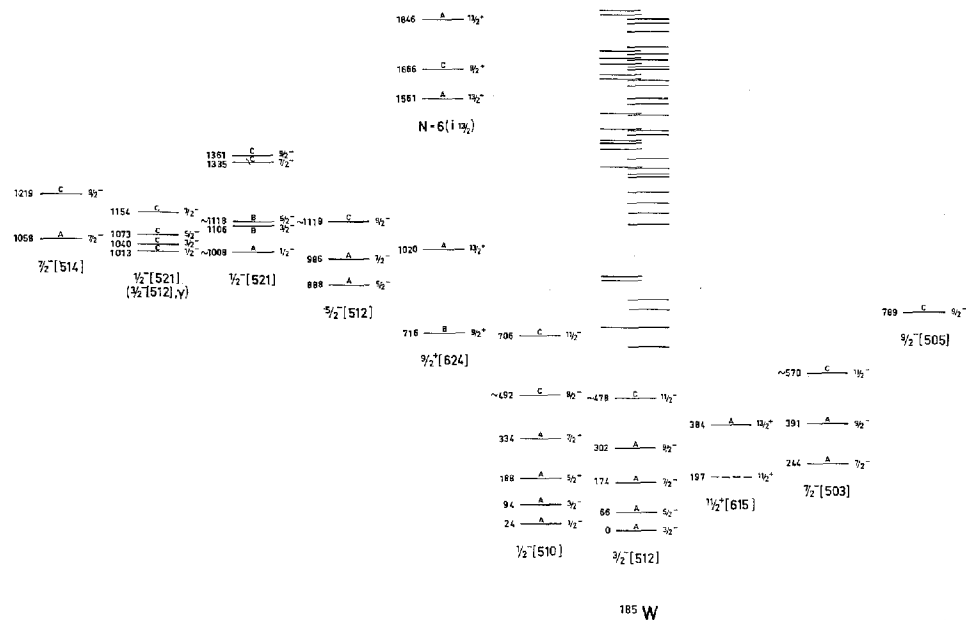


Fig. 13. Level scheme for ^{185}W . See caption to Fig. 10.

orbital and one therefore expects to observe six $13/2+$ states in a pick-up reaction. However, at excitation energies up to 4 MeV only four $13/2+$ states appear in the $(^3\text{He}, \alpha)$ spectra for ^{185}W and ^{183}W , and only two for ^{181}W where the Fermi surface is closer to the $9/2+[624]$ orbital. The total observed $l = 6$ cross section, though, in each case sums up to the total cross section predicted for all the $13/2+$ states.

A mixing calculation¹¹⁾ starting from a conventional Nilsson model does not remotely reproduce either the energies or cross sections, or even the number of states observed. Furthermore, it is easily seen that the alteration required is a general compression of the unperturbed energy spacings for the low K -value orbitals. Nilsson model calculations which include a hexadecapole or ϵ_4 deformation³⁴⁾ demonstrate that the energies for those orbitals in the wolfram region are indeed strongly compressed relative to the case with $\epsilon_4 = 0$. A Coriolis mixing calculation using the band head energies calculated from the Nilsson model with inclusion of an ϵ_4 deformation ($\epsilon_4 = +0.06$) correctly accounts for the observed number of states in ^{183}W and ^{185}W and gives reasonable values for energies and cross sections. In ^{181}W it predicts three states with strong population¹¹⁾.

Due to the reduced energy spacing, the higher lying orbitals mix more

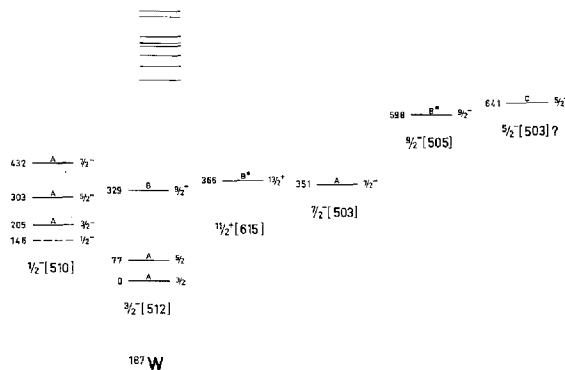


Fig. 14. Level scheme for ^{187}W . See caption to Fig. 10. The assignments of the two levels labeled B* may be reversed (cf. Sect. 4.7).

strongly and hence lose essentially all their cross section. The experimental energies for all three nuclei could be reproduced almost exactly by only minor alterations of the Nilsson model³⁴⁾ single particle energy spacings. The calculated cross sections are then also in good agreement with experiment.

Hexadecapole deformations have previously been established from inelastic scattering of deuterons³⁵⁾ and, more recently, of α -particles³⁶⁾. The evidence adduced here is an independent confirmation as it does not depend on the details of the reaction mechanism but only on the single particle level energy spacings and the relative sizes of cross sections.

Coriolis fits to the $13/2+$ states identified and to other $N = 6$ states known from previous studies of the wolfram nuclei suggested approximate energies for the $9/2+$ band members which are the only additional states expected with measurable cross sections. Because of the strong mixing there are usually few such states, and it was possible in most cases to locate corresponding groups in the spectra.

In ^{179}W , where no ($^3\text{He}, \alpha$) data are available, the lowest lying $13/2+$ state is observed at 468 keV by the (d, t) reaction with at least twice the cross section for a pure Nilsson state. A similar (d, t) cross section enhancement is observed for the lowest $13/2+$ state in the other wolfram nuclei. The $9/2$ and $11/2$ members of the $9/2+[624]$ band in ^{179}W have been previously²³⁾ placed at 308.7 keV and 421.2 keV. The latter of these states is, however, not confirmed in a recent study³⁷⁾ of the $^{178}\text{Hf}(\alpha, 3n\gamma)^{179}\text{W}$ reaction.

In ^{181}W , where the $9/2+[624]$ orbital is the ground state, only two $13/2+$ states are observed, at 250 keV and 1124 keV, but with a cross section sum

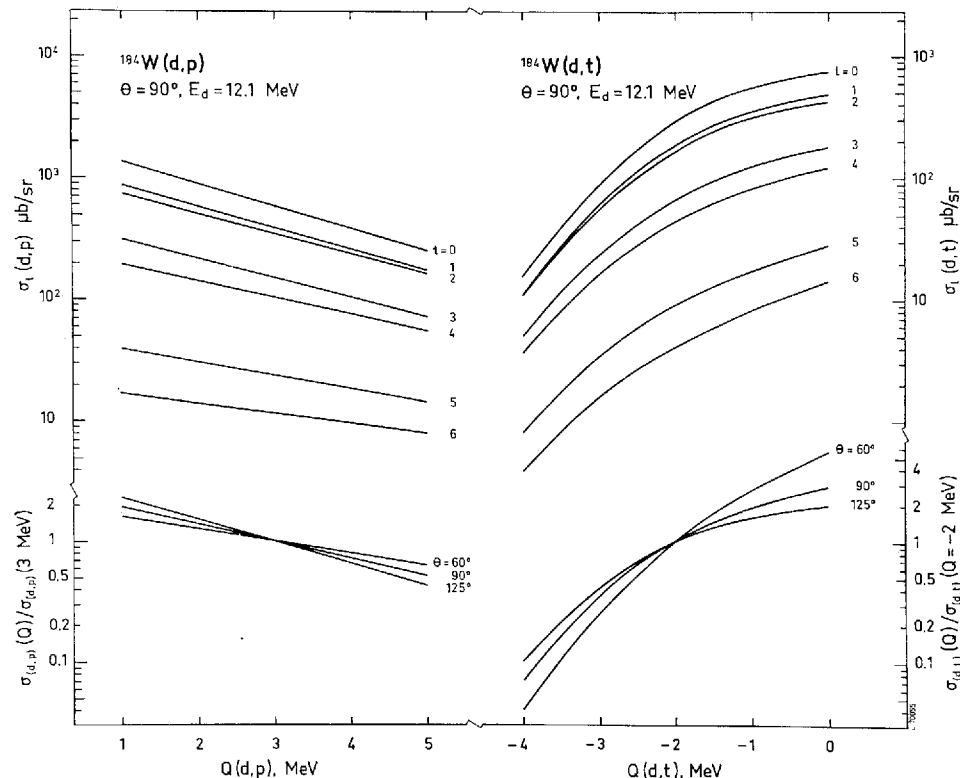


Fig. 15. Theoretical Q -dependence of the transfer reaction cross sections. The average Q -dependence used for Q -reduction of the measured cross sections is shown in the lower part of the figure.

corresponding to that of the five $13/2+$ hole states expected. A $7/2+$ state at 954 keV has been assigned in decay studies²⁴⁾ and a $9/2+$ state at 996 keV has been tentatively assigned on the basis of the coupling calculations¹¹⁾.

In ^{183}W and ^{185}W four $13/2+$ states have been identified as mentioned above. Also, the $9/2+[624]$ band head is clearly observed in the spectra for both nuclei. The state was known previously²⁵⁾ in ^{183}W , and it was here identified in ^{185}W at 716 keV (cf. sect. 4.7.). In each nucleus, one further $9/2+$ state has been tentatively assigned mainly on the basis of the calculations. The $11/2+[615]$ band head was known previously from radioactive decay studies^{25, 26)} in both nuclei.

The states of ^{187}W could not be studied by pick-up reactions. The position of the lowest $13/2+$ state is discussed in sect. 4.7.

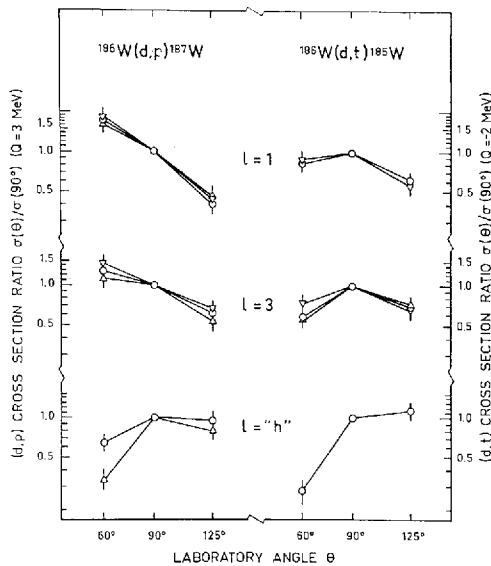


Fig. 16. The reduced cross section angular distributions for previously assigned states populated with $\sigma_{\text{exp}}(90^\circ) > 20 \mu\text{b}/\text{sr}$ in the (d,p) and (d,t) reactions on the ^{186}W target.

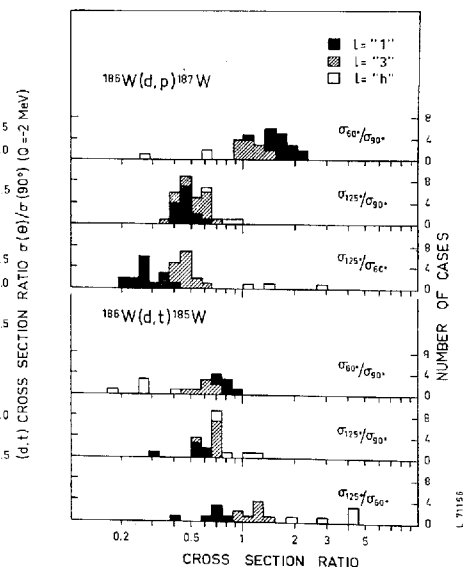


Fig. 17. The reduced cross section angular distributions for all states populated with $\sigma_{\text{exp}}(90^\circ) > 20 \mu\text{b}/\text{sr}$ in the (d,p) and (d,t) reactions on the ^{186}W target. The inferred l -transfer values are indicated.

4.9. High-lying Particle Excitations

As discussed in the preceding sections the majority of groups observed below 1 MeV of excitation can be explained in a quantitative manner. Only a few groups of appreciable intensity remain unassigned, e.g. the 666 keV and 733 keV levels in ^{185}W which are populated strongly in both the (d,p) and (d,t) reactions.

As mentioned earlier, the Nilsson model predicts a distinct energy gap above neutron number 118 and this is reflected in the corresponding region of all the (d,p) spectra by a sharp reduction in level density. A number of unassigned groups above this energy gap suggests possible fractionation of strong particle excitations. Several such excitations are expected according to the Nilsson model among which are the orbitals $1/2 + [651]$, $3/2 + [642]$, $3/2 - [501]$, $5/2 - [503]$ and $1/2 - [501]$. Of these, the two positive parity orbitals arising from the $g_{9/2}$ spherical state have generally been difficult to locate although a few tentative identifications have been made in rare earth nuclei²⁾. The difficulties may be partly attributed to the fact that Nilsson model predictions for these orbitals are highly sensitive to the values of the

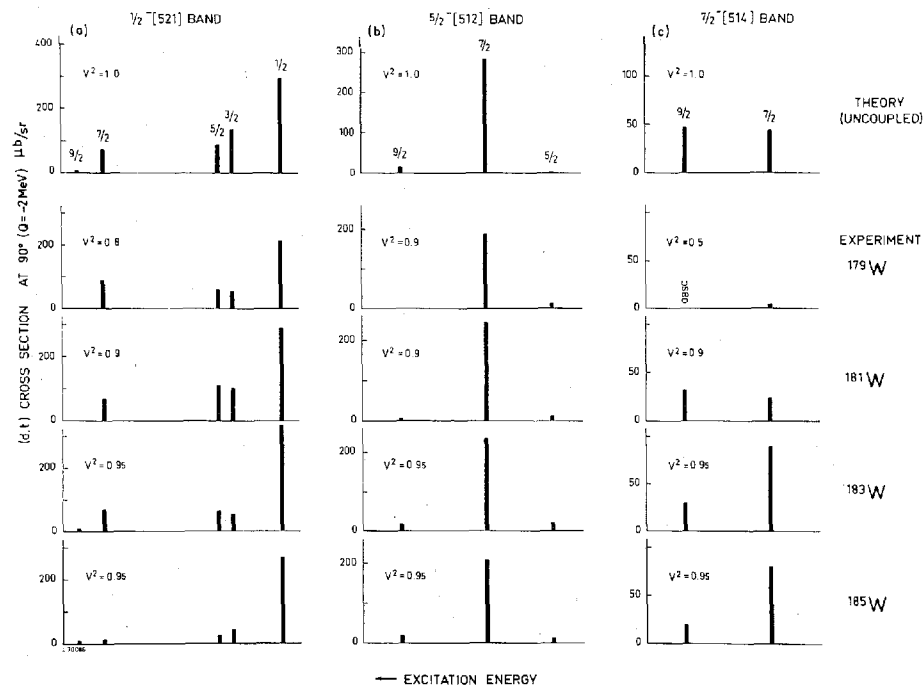


Fig. 18. (a), (b) and (c). Theoretical and experimental intensity patterns for the $1/2$ -[521], $5/2$ -[512], and $7/2$ -[514] bands in the odd W nuclei.

parameters δ , κ and μ adopted. Calculations^{38) 34)} with slightly different κ - and μ -values lead to entirely dissimilar fingerprint patterns (fig. 20). The Coriolis matrix element between the bands and the value of the decoupling parameter for the $K = 1/2$ band are also drastically affected by the choice of Nilsson parameters. The most substantial evidence for the identification of these orbitals is available for the ^{175}Yb nucleus³⁹⁾ where the two bands are located 500 to 1000 keV above the $3/2$ -[512] band. In the less deformed wolfram nuclei, the bands are expected to lie even higher above the $3/2$ -[512] band than in ^{175}Yb and accordingly it seems likely that some of the unassigned (d,p) groups in the 1 to 2 MeV excitation energy range correspond to members of the bands in question. A recent (p,p') study⁴⁰⁾ indicates an excitation energy of approximately 1300 keV for the $g_{9/2}$ strength in ^{185}W . However, no specific assignments have been possible, partly because of the aforementioned uncertainties in band characteristics and partly because our angular distribution results do not clearly indicate the parity of the observed states.

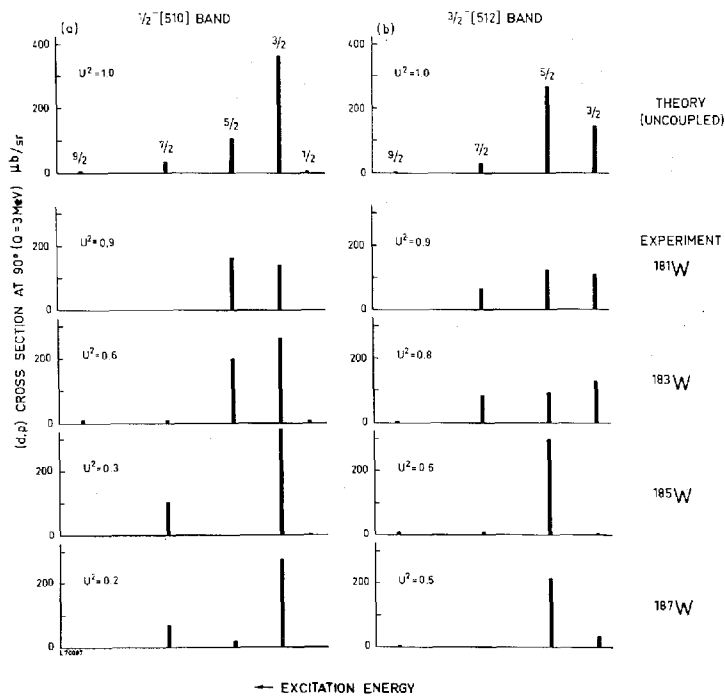


Fig. 19. (a) and (b). Theoretical and experimental intensity patterns for the $1/2-[510]$ and $3/2-[512]$ bands in the odd W nuclei.

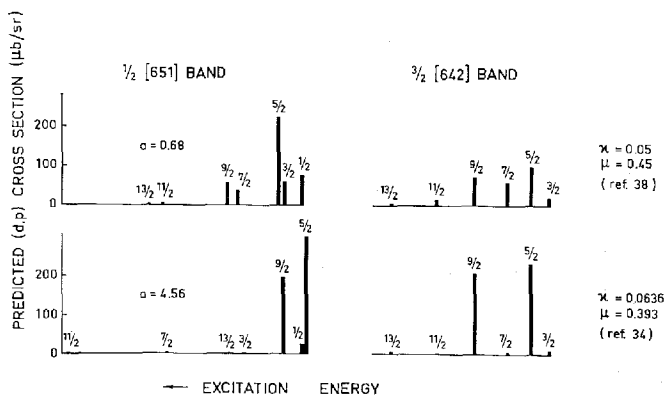


Fig. 20. Fingerprint patterns for the $1/2+[651]$ and $3/2+[642]$ bands calculated using the Nilsson model parameters of Refs. 38 and 34.

In contrast to the orbitals just discussed, the $3/2 - [501]$, $5/2 - [503]$ and $1/2 - [501]$ orbitals all converge towards lower energies with decreasing nuclear deformation. Very large (d,p) cross sections (500 to 1000 $\mu b/sr$) are predicted for these states and the corresponding groups should be expected to appear prominently in the (d,p) spectra. In fact, none of the unexplained peaks in the spectra exceeds 300 $\mu b/sr$. The only conclusion which can be drawn from the data is that the strength of these orbitals is spread over several groups. It should be noted that bands tentatively identified with the $3/2 - [501]$ orbital in hafnium⁴¹⁾ and osmium⁴²⁾ nuclei are populated with (d,p) cross sections considerably smaller than those predicted for this band.

Arguments can be made in favour of interpreting the 641 keV state in ¹⁸⁷W as the $5/2 - [503]$ band head. The results of a neutron capture gamma-ray study³⁰⁾ provide support for the assignment, as the state in question was observed to de-excite predominantly to the $7/2$ $7/2 - [503]$ level; in addition preliminary results⁴³⁾ of a (d,p) study using polarized deuterons indicate $I^\pi = 5/2 -$ for that state. However, the (d,p) cross section is five times lower than predicted and for this reason the assignment cannot be made with conviction.

The apparent fractionation of the high-lying $N = 5$ particle excitations seems to be a quite general feature for the hafnium, wolfram and osmium nuclei^{41, 42)}. It is probably significant that at the deformations of these nuclei the three pairs of quasi-intersecting orbitals $3/2 - [501] - 3/2 - [761]$, $5/2 - [503] - 5/2 - [752]$ and $1/2 - [501] - 1/2 - [770]$ occur close together. A recent theoretical study⁴⁴⁾ of $\Delta N = 2$ mixing in which a hexadecapole term was included in the nuclear deformation indicates that very strong mixing occurs between these pairs of orbitals in the wolfram region which may in part be the explanation for the observed fractionation.

4.10. Comparison of Experimental and Calculated Transfer Strengths

An overall measure of the agreement between the experimental data and the DWBA predictions is obtained by comparing the total observed cross section to the values calculated for these states. This comparison is given in table 9. The ratios S of the observed and theoretical cross sections for the individual Nilsson orbitals are calculated from the total cross section into all rotational members of each particular band; the effects of Coriolis mixing are included in these numbers. More detailed results for the individual band members are contained in tables 13 to 17.

As was discussed in the preceding section it was not possible to locate the higher lying particle excitations expected from the Nilsson diagram. The

TABLE 9. Ratios $S = \sigma_{90^\circ}^{exp}/\sigma_{90^\circ}^{calc}$ of experimental and calculated cross section for the $N = 5$ Nilsson orbitals.

Nilsson orbital	$S(d,p)$				$S(d,t)$			
	^{181}W	^{183}W	^{185}W	^{187}W	^{179}W	^{181}W	^{183}W	^{185}W
9/2 - [505].....	-	0.38	0.40	0.52	-	-	-	(2.5) ^a
7/2 - [503].....	0.91	0.77	0.91	0.57	-	1.07	1.44	2.13
3/2 - [512].....	0.64	0.72	1.13	1.07	-	1.33	1.23	1.22
1/2 - [510].....	0.55	1.10	1.58	2.05	1.02	0.24	1.07	0.89
5/2 - [512].....	0.56	(4.0) ^a	(3.9) ^a	-	0.76	0.91	1.14	1.03
1/2 - [521].....	1.04	(1.0) ^a	(<2.7) ^a	-	0.85	1.06	1.01	0.67
7/2 - [514].....	<0.3	(2.9) ^a	(3.0) ^a	-	obsc	0.74	1.14	0.82
Total ^b	0.70	0.88	1.15	1.03	0.82	0.92	1.09	0.93

^a The numbers in brackets refer to Nilsson bands which by the particular reaction are weakly populated.

^b The S -values given in this line refer to the total cross section for all assigned groups.

experimental data show an increased (d,p) strength for the higher mass numbers suggesting that these orbitals lie highest in ^{183}W . The total unassigned 90° , Q -reduced (d,p) cross section below 2 MeV of excitation is 1.5 mb, 2.1 mb, and 2.7 mb in ^{183}W , ^{185}W , and ^{187}W , respectively.

4.11. Single Particle Level Scheme

All Nilsson orbitals identified are compiled in fig. 21 which gives the band head excitation energies in the different wolfram nuclei. Particle excitations are shown above, hole excitations below the ground state. Except for the hole states in ^{179}W the Nilsson states occur in a fairly regular sequence.

An attempt to extract the corresponding single particle level schemes is shown in fig. 22 where the nuclei are arranged in order of increasing deformation. Also shown are the Nilsson model predictions³⁴⁾ for ^{187}W and ^{179}W . The experimental level schemes were placed such that the 1/2 - [510] orbital varies smoothly in energy from ^{187}W to ^{179}W . The experimental single particle energy spacings were obtained by eq. (3) from the band head excitation energies, corrected for the (usually small) effects of Coriolis mixing and from the adopted Fermi surface locations discussed in sect. 5.2. Since the latter could be determined only approximately, the level spacings close to the Fermi surface might not be very accurate. The rather irregular behaviour of the 9/2 + [624] and 7/2 - [514] orbitals might in part be at

tributed to such uncertainties. However, the discontinuities of the deeper lying hole states cannot be explained in that way.

The variation in the energy spacing of the $7/2 - [503]$ orbital relative to the $3/2 - [512]$ and $1/2 - [510]$ orbitals is somewhat unexpected. In contrast to predictions this spacing decreases towards larger deformations; in ^{181}W the $7/2 - [503]$ state even lies below the $3/2 - [512]$ orbital. This result may be related to the hexadecapole contribution to the nuclear deformation. It is noted that two recent theoretical investigations^{34, 45)} appear to lead to conflicting conclusions as to the relative variation of the hexadecapole term in the wolfram nuclei, which result in opposite trends for the $7/2 - [503]$ single particle energy through these nuclei. The observed energy variation is in accord with a hexadecapole term increasing towards higher mass numbers as predicted in ref.⁴⁵⁾. A similar variation of the hexadecapole term is indicated by the results of a recent (d, d') study⁴⁶⁾.

5. Coriolis Coupling of the $N = 5$ Orbitals

The Coriolis mixing calculations discussed here concern the odd parity $N = 5$ Nilsson orbitals*. These orbitals, which were treated separately in sects. 4.1 to 4.7, are coupled with matrix elements which typically are of the order of 100 keV. As the seven orbitals considered are observed within a range of excitation of approximately 1 MeV, it is clear that the coupling in several cases will be of decisive importance for the observed spectra. The values of $\langle |j-| \rangle$ entering the matrix elements of eq. (7) for the orbitals of the wolfram region are compiled in table 10.

TABLE 10. Theoretical values of $\langle K|j-|K+1 \rangle$ and of $-a_{1/2}$ for the orbitals identified in the wolfram nuclei.

(The Nilsson model parameters are $\delta = 0.22$, $\kappa = 0.0637$, $\mu = 0.42^{48)}$.

	$9/2 - [505]$	$7/2 - [503]$	$3/2 - [512]$	$1/2 - [510]$	$5/2 - [512]$	$1/2 - [521]$	$7/2 - [514]$
$9/2 - [505]$		-0.973					2.847
$7/2 - [503]$	-0.973				2.858		
$3/2 - [512]$				0.951	0.045	2.546	
$1/2 - [510]$			0.951	-0.003		-2.541	
$5/2 - [512]$		2.858	0.045				-1.151
$1/2 - [521]$			2.546	-2.541		-0.848	
$7/2 - [514]$	2.847				-1.151		

* Some of the results discussed in this section have been reported previously⁴⁷⁾.

The wolfram nuclei are favourable for an extensive test of the mixing effects because of the completeness of the experimental material. Thus all the odd parity orbitals expected from the Nilsson diagram have been identified, and energies and cross sections are known for about 20 levels of these odd parity bands in each nucleus.

In the mixing calculations, the unperturbed band head energy, the rotational energy parameter A_K and the decoupling parameter $a_{1/2}$ for each band were considered as unknowns to be determined from the experimental level energies. The Coriolis coupling matrix elements on the other hand, were fixed by the Nilsson value (eq. (7)) with definite prescriptions for the empirical attenuation coefficients η which will be discussed below. The number of experimentally known level energies always exceeded the number of unknowns. Final values for the unperturbed band head energies and rotational parameters were determined by a fitting procedure which was interrupted when the level energies were reproduced to within an accuracy of about 1 keV. The most stringent test of the calculations centred on the comparison of the experimental cross sections with those calculated using the mixed wave functions obtained by fitting the excitation energies.

5.1. Methods of Calculations

The Coriolis coupling calculations were performed with an Algol code that diagonalized the interaction matrix and calculated the perturbed energy eigenvalues and wave functions as well as the transfer reaction cross sections. The input includes the single particle cross sections φ_l and the inertial strength parameter $\hbar^2/2\mathfrak{J}$ entering the matrix elements as well as, for each band, the band head energy, the rotational energy parameters A_K and $a_{1/2}$, the empirical attenuation factor η_K , the occupation amplitudes U and V , and the Nilsson wave function. The inertial strength parameter $\hbar^2/2\mathfrak{J}$ is taken as the average of the values derived from the $2+$ energies in the neighbouring even nuclei. The occupation amplitudes were calculated for each orbital from the unperturbed band head energies and the Fermi surface location λ by eqs. (3) and (4). The Nilsson wave functions used were those calculated for the Nilsson parameters $\delta = 0.22$, $\kappa = 0.0637$ and $\mu = 0.420$ ⁴⁸⁾.

All the observed negative parity bands were included in the calculations (see fig. 21 for the bands included for each nucleus). Tests were made of the effects of unobserved bands by including them in separate calculations both at their Nilsson energies and at strongly reduced energies and with exaggerated coupling strengths to obtain limits on their effects. Only

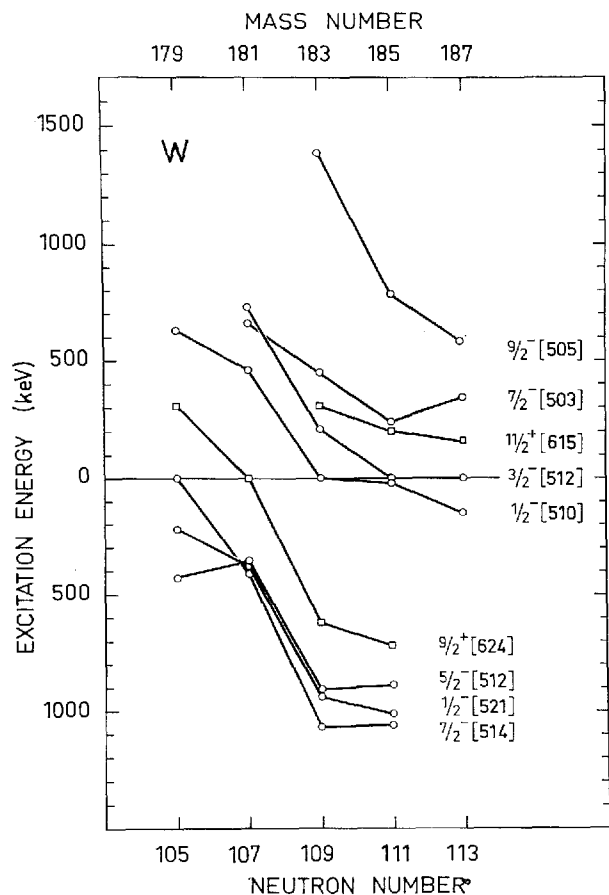


Fig. 21. Bandhead energies of the Nilsson orbitals identified by neutron transfer. Points at negative energies indicate hole states.

the $5/2^-$ - [523] band had appreciable effects on the lower lying levels and even here no serious alterations occurred.

5.2. Fermi Surface Location

As the coupling matrix elements and the calculated cross sections both depend on the U 's and V 's, it was necessary to estimate the energy λ of the Fermi surface for each nucleus. The convenient prescription locating it at the ground state proved to be insufficient for the low lying orbitals. The Fermi surfaces were approximately determined by comparing ratios of ex-

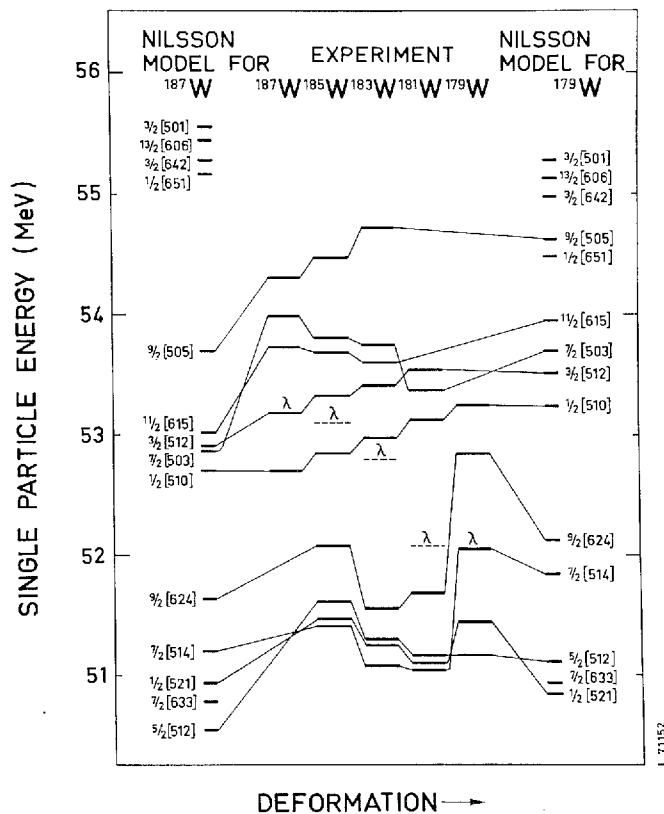


Fig. 22. Single particle level schemes for the odd W nuclei extracted from the experimental bandhead energies and the adopted Fermi surface locations. The Nilsson model predictions are from Ref. 34.

perimental (d,p) and (d,t) cross sections for certain low lying states with the theoretical values calculated as a function of the parameter λ . The levels chosen for these determinations were those least affected by mixing from high lying states and with large and accurately known cross sections. As the low lying states themselves are usually strongly mixed, the theoretical ratios had to be evaluated with all mixing effects included.

The procedure used is illustrated in fig. 23 for the ^{183}W nucleus. In this case the most suitable states are the $3/2\ 1/2-[510]$ and $5/2\ 1/2-[510]$ states, and in the figure the experimental and calculated ratios of (d,t) to (d,p) cross sections for these states are compared. The results indicate that in this nucleus the Fermi surface is located about 150 keV below the

1/2 - [510] band head. A similar procedure was used in the cases of ^{181}W and ^{185}W . No (d,p) data are available for ^{179}W and so the Fermi surface was placed at the ground state; since, however, essentially no mixing occurs in this nucleus the placement is not crucial. In ^{187}W where no (d,t) data exist, the Fermi surface was also placed at the ground state. The adopted Fermi surface locations which were subsequently used in all calculations are indicated in fig. 22.

5.3. Empirical Coriolis Coupling Strength

As mentioned in sect. 2, it has empirically been found that the Coriolis matrix elements calculated from the Nilsson model generally are too large. Hence the attenuation factors η_K were introduced in eq. (7). The product $\eta_K \cdot \eta_{K+1}$ is the attenuation for the Nilsson coupling strength between the orbitals with projection quantum numbers K and $K+1$. As already mentioned the inertial strength parameter $\hbar^2/2\mathfrak{J}$ also entering in (7) was kept at its value in the even isotopes, and all deviations between theory and experiment are thus included in the $\eta_K \cdot \eta_{K+1}$ factor.

Fits to the observed energies were attempted with a variety of attenuation prescriptions, and the calculated cross sections were compared to experiment. Semiquantitative criteria for good and bad agreement between theoretical and experimental cross sections were adopted and these were used consistently in judging whether the execution of a new calculation had brought about an overall improved agreement between theory and experiment. In this way the attenuation factors to be discussed below were arrived at.

Initial coupling calculations performed with full coupling strength ($\eta_K \cdot \eta_{K+1} = 1$) in ^{183}W and ^{185}W gave good agreement with experimental results for the strongly mixed low lying 1/2 - [510] and 3/2 - [512] bands. However, difficulties were encountered for several high lying states in these nuclei; although the inclusion of mixing improved the agreement between calculated and experimental cross sections, it was impossible to reproduce the experimental energies. Calculations performed at half and quarter strengths (i.e. $\eta_K \cdot \eta_{K+1} = 0.5$ and 0.25) did reproduce the experimental energies and also the cross section agreement was improved. Still better agreement was, however, obtained by the use of full strength for all matrix elements except those involving either or both the 7/2 - [514] and 5/2 - [512] bands. In the wolfram nuclei the latter two orbitals predominantly mix with each other and the ratio of transfer cross sections for their 7/2 - states is critically dependent upon the amount of mutual mixing. In order to re-

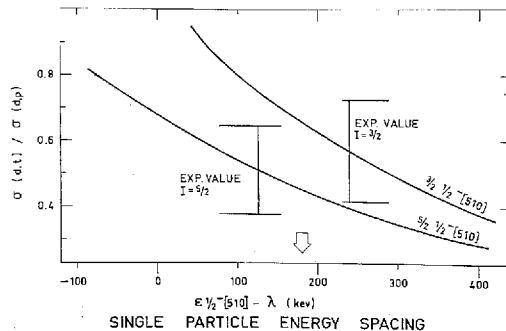


Fig. 23. Fermi surface location in ^{183}W . The result is indicated by an arrow.

produce the experimental cross sections for these two $7/2^-$ states in ^{183}W and ^{185}W , a rather strong attenuation ($\eta_{5/2} \cdot \eta_{7/2} = 0.25$) is required. A good overall description for the experimental data in ^{183}W was obtained by using full coupling strength for all matrix elements except those involving the two orbitals mentioned which were each kept at an attenuation of $\eta = 0.5$. An identical procedure also gave good results for ^{185}W where the Nilsson states occur at similar excitation energies as in ^{183}W .

For both nuclei slightly better results were actually obtained if the matrix elements connecting the $1/2^-$ -[521] orbital with the bands in the ground state region were also reduced. This reduction, however, arises naturally out of the attenuation prescription which subsequently evolved and was finally adopted.

However, application of the same attenuations in ^{181}W gave very poor results. In this nucleus, the $5/2^-$ -[512] and $7/2^-$ -[514] bands occur at about 400 keV excitation, and the strongly attenuated coupling strength ($\eta_{5/2} \cdot \eta_{7/2} = 0.25$) required in ^{183}W and ^{185}W could not bring the calculated cross sections into agreement with the data; a smaller reduction in coupling strength was indicated ($\eta_{5/2} \cdot \eta_{7/2} \approx 0.50$). In addition, the coupling strength for the $1/2^-$ -[510] and $1/2^-$ -[521] bands which also occur close together at about 400 keV excitation in ^{181}W had to be substantially attenuated in order to obtain even fair agreement with experiment.

The required attenuations for the pairs of orbitals just discussed are shown in fig. 24 a. These results suggest that the same matrix element requires different attenuations in different nuclei. Guided by the results shown in fig. 24 a, we therefore performed coupling calculations in which each wave function was attenuated with an η_K decreasing linearly with the excitation energy of the band head. The specific slope chosen was determined

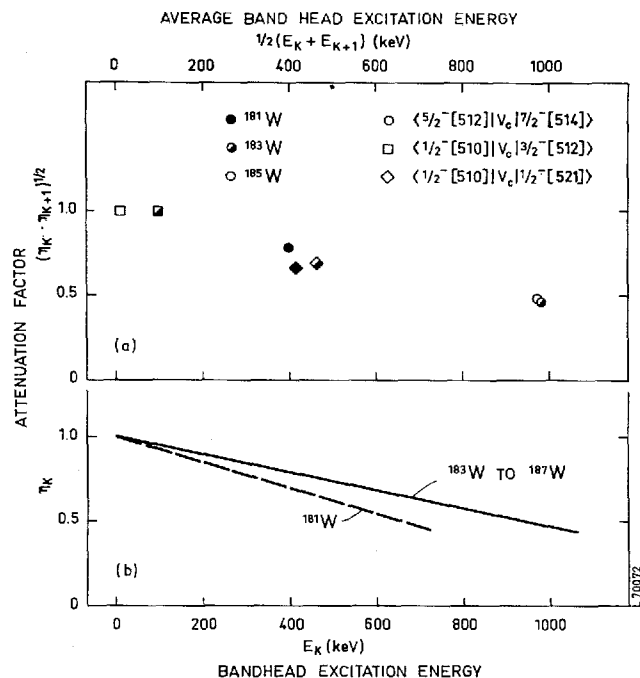


Fig. 24. (a) Empirical Coriolis matrix-element attenuation factors in different wolfram nuclei shown as a function of the average excitation energy of the two admixed bands. (b) Energy dependence of the attenuation factors η_K adopted in the coupling calculations.

by requiring that the calculated ratio of (d,t) cross sections into the $7/2^- [514]$ and $7/2^- [512]$ states in ^{183}W should be identical to the measured ratio. With the η_K fixed by this prescription, an identical energy dependence was used for $^{179}, ^{183}\text{--}^{187}\text{W}$; a slightly stronger decrease was optimal for ^{181}W (see fig. 24 b). The same empirical rule for η_K also gave optimal results for the positive parity states in these nuclei¹¹). Other prescriptions for the η_K factors also yield improved agreement with experiment but the best agreement was obtained with that described here.

The adopted attenuation prescription is arbitrary to the extent that it is based on the transfer cross sections to two particular strongly coupled states. Indeed our analysis leaves unexplained appreciable systematic deviations between experimental and calculated cross sections for a few other states. That no such deviations occur for the two crucial $7/2^-$ states was inherently assumed in arriving at the specific attenuation prescription. In

$^{186}\text{W}(d,t)^{185}\text{W}$
 $\theta = 90^\circ$ $Q = -2 \text{ MeV}$

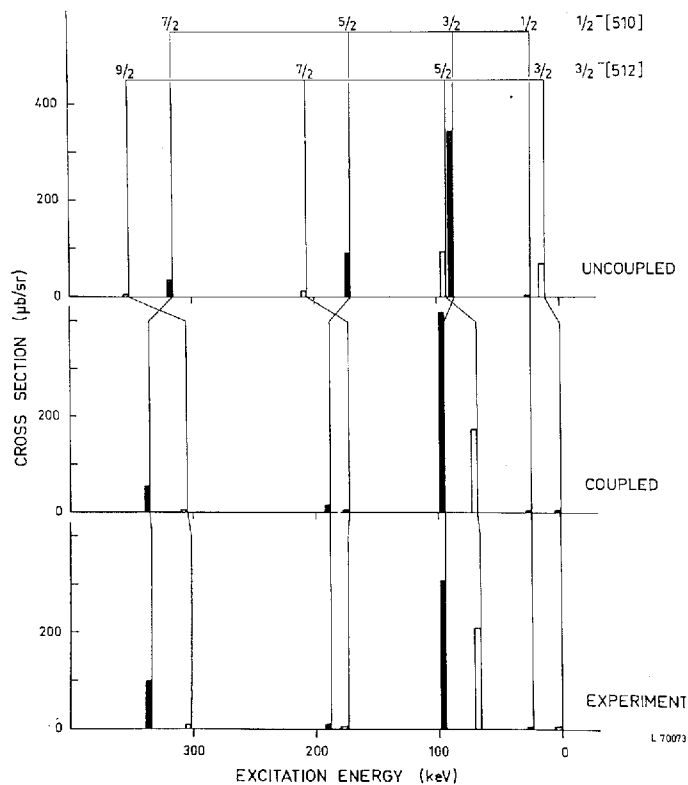


Fig. 25. Calculated and experimental (d,t) cross sections for the $1/2$ -[510] and $3/2$ -[512] bands in ^{186}W .

any case, it is clear that certain matrix elements must be substantially attenuated in order to reproduce the observed energies and cross sections.

At present, the origin of this attenuation and the variation in different nuclei is not understood, but the prescription adopted here might be given the physical rationale that small contributions from many higher lying unobserved bands not included among the basis states tend to affect the observed states at higher excitation energy more than those near the ground state. A difficulty, however, is that an attenuation of the decoupling parameter for the $1/2$ -[521] band is not simultaneously observed, nor are the cross sections for high lying bands generally diminished. It may be best to treat the above prescription as only an empirical rule; it may merely sim-

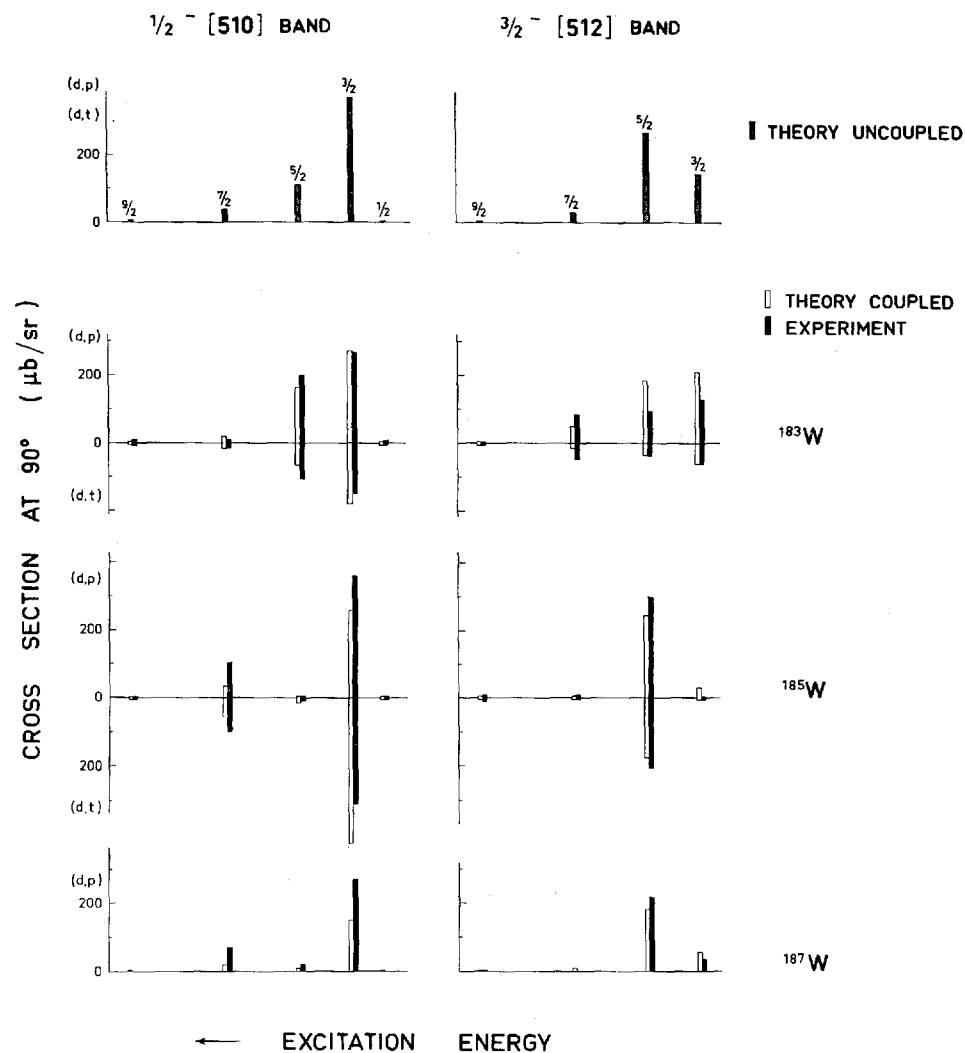


Fig. 26. Calculated and experimental cross sections for the $1/2-[510]$ and $3/2-[512]$ bands in ^{183}W , ^{185}W and ^{187}W . The unperturbed fingerprint patterns which are essentially identical for both the (d,p) and (d,t) reactions are shown above. (In ^{187}W the $1/2\ 1/2-[510]$ and $7/2\ 3/2-[512]$ state were not observed; the experimental (d,p) cross sections are less than $8\ \mu\text{b/sr}$).

ulate a dependence of the Coriolis coupling strength on parameters not considered in the present calculations.

Once the attenuation prescription was chosen, the coupling calculations

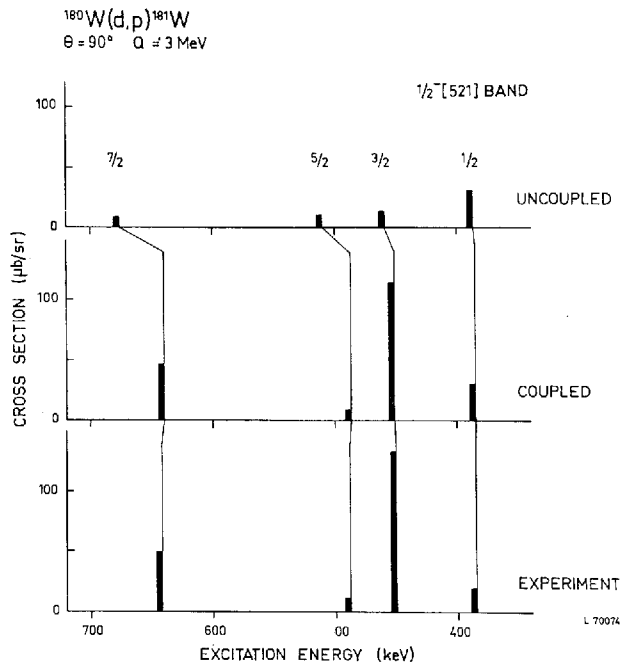


Fig. 27. Calculated and experimental (d,p) cross sections for the $1/2^- [521]$ band in ^{181}W .

were performed to reproduce the observed excitation energies only. Using the wave functions obtained from this energy fit, and with no further variation of parameters, the cross sections were calculated and compared with the experimental values. The results are given in the following section.

5.4. Analysis of Results for Coriolis Coupled Bands

All the unperturbed, the Coriolis perturbed, and the measured energies and cross sections are given in tables 13 to 17 to which reference should be made for numerical results. The figures discussed below illustrate some of the more striking consequences of the mixing.

As was mentioned in sect. 4 it is often found that the experimentally observed fingerprint patterns bear little resemblance to those calculated with no mixing included (cf. figs. 18 and 19). A specific example, the (d,t) cross sections for the $1/2^- [510]$ and $3/2^- [512]$ bands in ^{185}W , is shown in fig. 25 where the inclusion of Coriolis mixing in the calculation brought about a spectacularly improved agreement between calculated and experimental cross sections. In this nucleus the effects of mixing are particularly

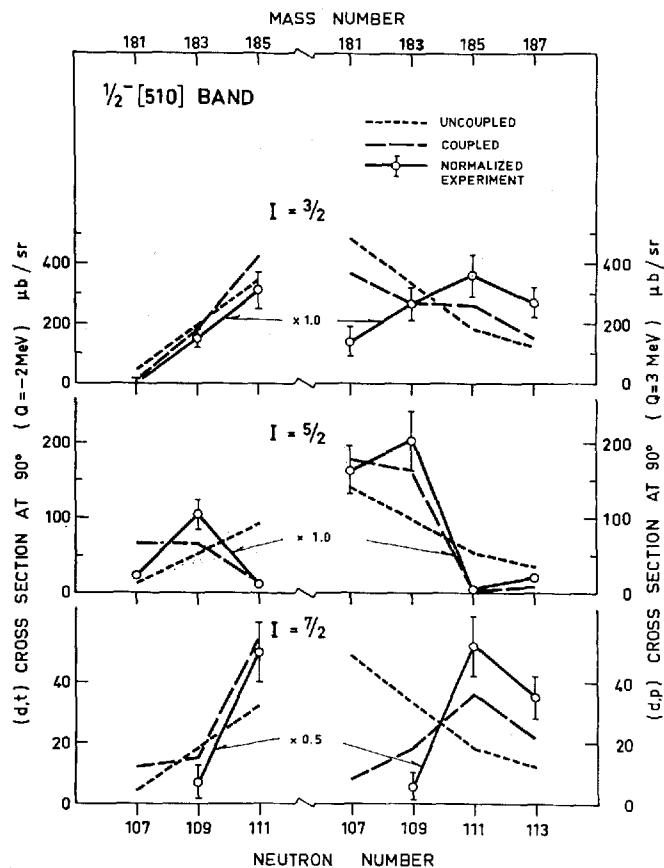


Fig. 28. Cross section systematics of members of the $3/2^-$ -[512] band in ^{181}W to ^{187}W . The experimental cross sections are normalized with the indicated multiplicative numbers (see discussion in Sect. 5.4).

drastic since the two bands lie very close together. In ^{183}W and ^{187}W , where these bands also occur at low excitation energies, the coupling calculations were similarly successful in accounting for all the observed cross sections (fig. 26).

Another example of Coriolis coupling having a striking influence on the population cross sections is seen in ^{181}W , where the $1/2^-$ -[510] and $1/2^-$ -[521] bands occur at similar excitation energies but on opposite sides of the Fermi surface. In the (d,p) spectra, the $3/2^-$ - and $7/2^-$ - members of the $1/2^-$ -[521] band are seen with much larger intensities than expected from pairing

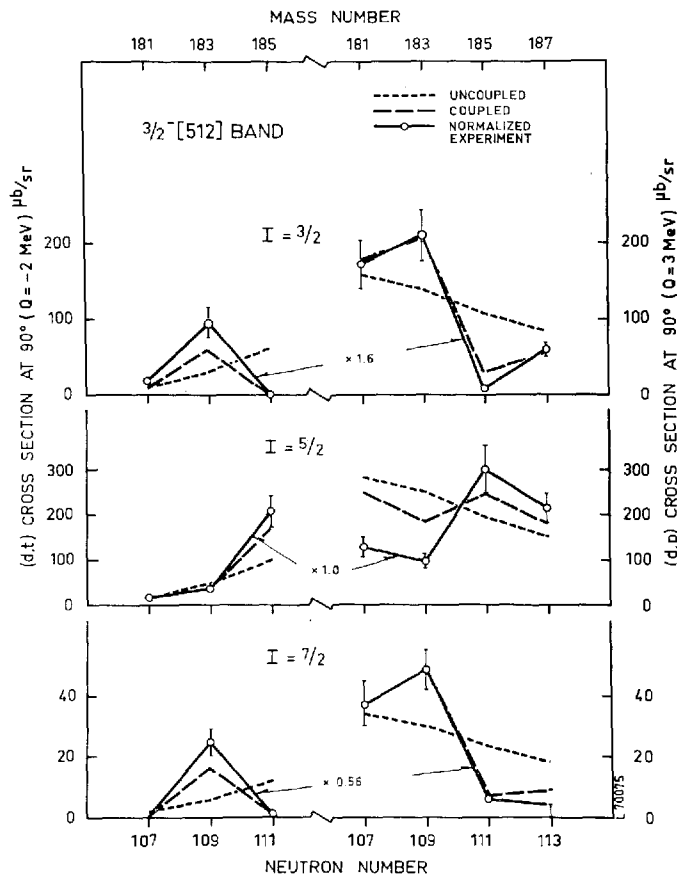


Fig. 29. Cross section systematics of members of the $1/2^-$ [510] band in ^{181}W to ^{187}W . See caption to Fig. 28.

theory while the $1/2^-$ and $5/2^-$ members have about the expected intensities. The two $K = 1/2$ bands are coupled by a fairly large matrix element and the resulting particle hole mixing effects are illustrated in fig. 27 for the (d,p) cross sections into the members of the $1/2^-$ [521] band. It is a consequence of the signs and relative magnitudes of the $C_{j\mu}$ coefficients and the mixing amplitudes that in this case only certain states are populated with large cross sections in both (d,p) and (d,t) reactions; the two cross sections arise from the different parts of the wave function which retain their respective occupation amplitudes in the mixed states. Some other features of the ^{181}W analysis are however less satisfactory, e.g. the anomalous

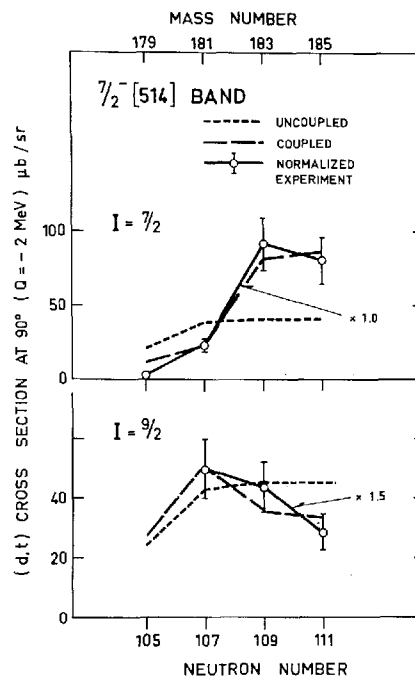


Fig. 30. Cross section systematics of members of the $7/2^- [514]$ band in ^{179}W to ^{185}W . See caption to Fig. 28.

decoupling parameters obtained for the unperturbed $K = 1/2$ bands (table 11). Even more disturbing is the poor agreement between calculation and experiment for the strongly populated $3/2^- 1/2^- [510]$ state (table 14). This disagreement is, in fact, the largest discrepancy between theory and experiment encountered in the present work and is probably not associated with Coriolis coupling.

It has been observed that the (d,t) cross sections for particle states and the (d,p) cross sections for hole states are generally larger than predicted by pairing theory (cf. table 9). These observations may reflect the individually small contributions from neglected states on the opposite of the Fermi surface.

An important aspect of this study is the investigation of certain coupling matrix elements in several nuclei. Due to the different relative excitation energies of the Nilsson bands the coupling of the same bands can give rise

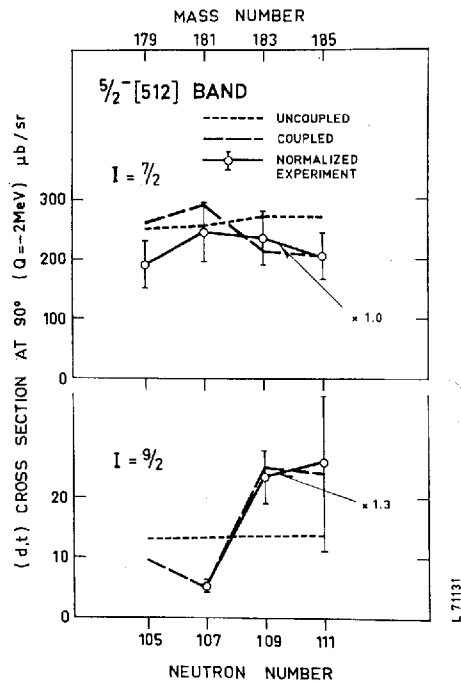


Fig. 31. Cross section systematics of members of the $5/2-[512]$ band in ^{179}W to ^{185}W . See caption to Fig. 28.

to distinctive cross section variations from nucleus to nucleus. Systematic cross section examinations of this kind tend to distinguish between coupling effects and deviations from theory arising from other sources; the latter are expected to vary little with mass number. It is indeed found that the absolute cross sections for certain states deviate systematically in all nuclei from the calculated values. The deviation may be due to deficiencies in the Nilsson wave functions or to second order (coupled channel) effects in the reaction mechanism. Empirical normalization factors were therefore applied in figs. 28 to 31 to remove these deviations.

The cross section systematics for the $3/2-[512]$ band and its prominent mixing partner, the $1/2-[510]$ band are shown in figs. 28 and 29. The pairing theory predicts a smooth cross section variation of about a factor two through the wolfram nuclei, whereas the observed cross sections vary by factors of 10 to 100. The sudden change in all cross sections from ^{183}W

TABLE 11. Observed and unperturbed energy parameters A_K , in keV, and $a_{1/2}$ (in paranthesis) for negative parity rotational bands in the wolfram nuclei.

Nilsson band	¹⁷⁹ W		¹⁸¹ W		¹⁸³ W		¹⁸⁵ W		¹⁸⁷ W	
	observed ^a	unperturbed								
7/2 - [503]					15.8	16.1	16.4	16.9		
3/2 - [512]			16.2	16.7	16.6	16.1	13.1	16.2	15.5	17.0
1/2 - [510]			15.0	13.1	13.0	14.4	21.1	18.8	19.7	17.6
			(0.59)	(0.71)	(0.19)	(0.16)	(0.11)	(0.09)	(0.00)	(-0.04)
5/2 - [512]	14.5	14.1	15.7	13.5	13.8	13.9	14.0	14.0		
1/2 - [521]	15.2	16.0	14.6	17.0	18.2	17.5	16.7	15.9		
	(0.82)	(0.79)	(0.48)	(0.40)	(0.70)	(0.72)	(0.86)	(0.90)		
7/2 - [514]	13.3	13.6	13.3	15.9	16.3	16.1	17.8	17.6		
A average	14.3	14.6	15.0	15.2	15.5	15.7	16.5	16.6	17.6	17.3
A even ^b		17.4		17.0		17.6		19.5		21.9

^a Extracted from experimental energies of lowest two (for $K = 1/2$ three) band members.

^b Average of A -values for the two neighbouring even nuclei.

to ¹⁸⁵W is caused by the interchange of the positions of the two orbitals. In ¹⁸¹W and ¹⁸³W, the 1/2 - [510] band lies below the 3/2 - [512] band while in ¹⁸⁵W and ¹⁸⁷W their positions are reversed. The Coriolis mixing merely gives rise to a redistribution of population cross section between the states of equal angular momentum I without altering the total cross section to that I . This feature is most readily seen for the $I = 5/2$ states of the two bands.

The 7/2 - [514] and 5/2 - [512] Nilsson orbitals, which form another pair of strongly coupled bands, are illustrated in figs. 30 and 31. The predominant feature of their mixing appears in the 7/2 - band members which have very different C_{jl} coefficients. The coupling therefore affects the 7/2 5/2 - [512] state, which has the large C_{jl} value, only slightly, while the same mixing amplitude causes a drastic cross section alteration for the 7/2 7/2 - [514] state.

A less specific but broader view of the Coriolis mixing is provided by the data shown in table 11. Here the rotational energy parameters for the negative parity bands in the wolfram nuclei are given together with the values for the corresponding unperturbed bands. Ideally the removal of

all coupling effects should cause the inertial parameters for the various bands to converge towards a single value. The fact that the unperturbed band parameters listed in the table are clearly more closely grouped than the perturbed values provides reassurance that the Coriolis coupling treatment used here is generally correct. The additional expectation that the inertial parameters of the decoupled bands should approach the value for the neighbouring even nucleus is realized to a much lesser extent. Although a slight tendency in that direction is discernible, the overall effect is less than startling. This particular departure from theoretical expectations has been observed in other nuclei⁴⁹⁾ and is not currently understood.

6. Conclusions

The level structure of the five odd mass wolfram nuclei ^{179}W to ^{187}W has been investigated by the (d,p) , (d,t) and $(^3\text{He},\alpha)$ neutron transfer reactions. The results considerably increase the knowledge about these nuclei and provide the material for a more detailed understanding of the single particle level structure over an energy range of about 4 MeV. All Nilsson states expected in this region have been identified.

A number of unassigned groups in the (d,p) spectra above ~ 1 MeV excitation energy suggest that the strong particle excitations expected above the $N = 118$ energy gap are fractionated; this phenomenon may be associated with strong $\Delta N = 2$ mixing.

A quantitative analysis of the Coriolis coupling between the $N = 5$ Nilsson orbitals has been performed. In most cases, the inclusion of the Coriolis interaction has greatly improved the agreement between calculated and experimental cross sections. In particular, several rather tentative assignments have been solidified by examining the effects of the mixing on the theoretical cross sections. The detailed analysis has revealed that overall satisfactory agreement can be obtained for both level energies and population cross sections only if certain coupling matrix elements are reduced below their Nilsson model values. An energy dependent systematic attenuation of the matrix elements which satisfactorily accounts for the experimental observations is suggested here, but other attenuation schemes are also feasible. Attempts⁵⁰⁾ to provide a theoretical basis for explaining the need for attenuated Coriolis matrix elements, revealed in these and in other experimental investigations, have not thus far been successful.

Acknowledgments

The authors wish to thank A. MØGELVANG for valuable help at various stages of this study, G. SIDENIUS for the fabrication of the mass separated targets and Mrs. G. DAM-JENSEN and Mrs. E. NIELSEN for their painstaking scanning of the plates. The assistance of C. NEWTON in the modification of the Coriolis mixing code is gratefully acknowledged. For their interest in this work and for many enlightening discussions we thank B. L. ANDERSEN, B. R. MOTTELSON, G. LØVHØIDEN, J. BANG and J. WADDINGTON. We express our appreciation of the excellent facilities and stimulating atmosphere at the Niels Bohr Institute. One of us (R.C.) acknowledges secretarial assistance provided by Los Alamos Scientific Laboratory, another (P.K.) acknowledges support from The Physics Laboratory, The Royal Veterinary University, Copenhagen, and a third (P.D.) acknowledges financial support from the U.S. Atomic Energy Commission and leave of absence from Purdue University.

7. Appendix

TABLE 12. Nilsson wave functions ($C_{j\ell}$ -values for the wolfram nuclei).
($\delta = 0.22$, $\kappa = 0.0637$, $\mu = 0.42^{48}$).

$K^\pi [Nn_z A]$	$C_{1/2,1}$	$C_{3/2,1}$	$C_{5/2,3}$	$C_{7/2,3}$	$C_{9/2,5}$	$C_{11/2,5}$
9/2 - [505]					0.9975	0.0713
7/2 - [503]				0.9367	-0.3358	0.0995
3/2 - [512]		0.3794	0.8153	0.2831	0.3275	0.0627
1/2 - [510]	0.0210	-0.6763	0.5862	-0.3427	0.2768	0.0671
5/2 - [512]			-0.0234	0.8362	-0.5249	0.1570
1/2 - [521]	-0.5101	0.3452	0.4726	0.4310	0.4440	0.1198
7/2 - [514]				0.3226	0.9378	0.1281

TABLE 13. Comparison of unperturbed, Coriolis coupled and experimental cross sections in ^{170}W ($\theta = 90^\circ$).

State ^a	Energy (keV)		$\sigma(d,t)$ $\mu\text{b}/\text{sr}$		
	Per- turbed	Exper- imental	Unper- turbed	Per- turbed	Exper- imental
1/2 1/2 - [510]	627		0.0	0.2	
3/2	689.3	689	10.5	28.9	22
5/2	788.0	788	10.9	19.4	27
5/2 5/2 - [512]	430.3	430.3	0.2	0.2	14
7/2	531.6	531.5	250.8	259.5	189
9/2	661.6		13.3	9.6	
1/2 1/2 - [521]	221.8	221.7	242.2	242.1	218
3/2	304.7	304.6	110.7	123.2	53
5/2	317.8	318.2	74.4	68.8	58
7/2	508.5	508.4	61.9	66.6	90
9/2	534.2	532.7	8.7	7.8	obsc
11/2	822.2	~ 816	0.6	0.6	~ 9
7/2 7/2 - [514]	0.0	0.0	21.1	12.2	~ 3
9/2	119.2	119.8	23.8	27.2	obsc
11/2	265.0	264.7	0.4	0.3	

^a Unestablished band members with calculated cross sections less than 1 $\mu\text{b}/\text{sr}$ are omitted.

TABLE 14. Comparison of unperturbed, Coriolis coupled and experimental cross sections in ^{181}W ($\theta = 90^\circ$).

State ^a	Energy (keV)		$\sigma(d,p)$ $\mu\text{b}/\text{sr}$			$\sigma(d,t)$ $\mu\text{b}/\text{sr}$		
	Per-turbed	Exper-imental	Unper-turbed	Per-turbed	Exper-imental	Unper-turbed	Per-turbed	Exper-imental
7/2 7/2 - [503] ..	661.8	661.8	373	316	296	24	2.7	45
9/2 ..	(813.3)		7	6		0.4	0	
3/2 3/2 - [512] ..	726.2	726.2	158	178	107	10	8	11
5/2 ..	811.0	807.3	284	251	126	16	10	13
7/2 ..	931.2	937	34	37	~ 67	1.9	0.3	
1/2 1/2 - [510] ..	457.6	457.6	0.5	0.1		0.0	6	
3/2 ..	529.6	529.3	485	365	~ 140	47	9	
5/2 ..	561.9	560.4	142	177	164	13	66	23
7/2 ..	729.8		49	8		4	12	
5/2 5/2 - [512] ..	365.5	365.5	0.0	0.0		0.2	0.2	11
7/2 ..	475.5	475.5	35	84	51	254	291	246
9/2 ..	618.0	~ 611	2.1	9	< 1	13	5	4
11/2 ..	792.6	777	0.2	0.1		1.2	0.1	7
1/2 1/2 - [521] ..	385.3	385.2	31	31	20	265	259	288
3/2 ..	450.8	450.2	14	114	135	121	161	95
5/2 ..	487.2	488.3	10	9	11	82	35	107
7/2 ..	639.5	642	9	46	~ 50	67	62	70
9/2 ..	804.1		1.4	7		10	8	
7/2 7/2 - [514] ..	409.2	409.0	5	12	< 3	38	23	23
9/2 ..	523.3	~ 527	6	0.1		43	51	33

^a Unestablished band members with calculated cross sections less than 1 $\mu\text{b}/\text{sr}$ are omitted.

TABLE 15. Comparison of unperturbed, Coriolis coupled and experimental cross sections in ^{183}W ($\theta = 90^\circ$).

State ^a	Energy (keV)		$\sigma(d,p)$ $\mu\text{b/sr}$			$\sigma(d,t)$ $\mu\text{b/sr}$		
	Per-turbed	Exper-imental	Unper-turbed	Per-turbed	Exper-imental	Unper-turbed	Per-turbed	Exper-imental
9/2 9/2 - [505] ..	1390.4	1390	64.0	64.6	25	1.8	1.2	
7/2 7/2 - [503] ..	453.1	453.1	357.3	363.7	284	37.6	48.3	72
9/2 ..	595.3	~ 596	7.0	8.0	~ 3	0.6	1.3	~ 1
3/2 3/2 - [512] ..	208.7	208.8	138.2	207.6	131 ^b	29.1	60.1	58 ^b
5/2 ..	292.5	291.7	248.8	184.0	96	48.1	34.4	35
7/2 ..	410.4	412.1	30.0	48.5	87	5.8	16.7	44
9/2 ..	556.3	~ 553	6.0	3.9	4	1.0	1.0	< 1
11/2 ..	740.0	742	0.2	0.4	4	0.0	0.1	1.3
1/2 1/2 - [510] ..	0.0	0.0	0.3	0.4	8	0.2	0.6	5
3/2 ..	45.1	46.5	334.0	268.9	264	194.9	178.5	150
5/2 ..	99.7	99.1	97.8	163.4	202	52.4	65.0	103
7/2 ..	207.5	207.0	33.4	17.7	11 ^b	17.9	15.0	14 ^b
9/2 ..	309.7	309.0	3.3	5.5	11	1.6	1.6	7
5/2 5/2 - [512] ..	905.8	906	0.0	0.0	6	0.2	0.2	19
7/2 ..	1002.5	1002	16.6	7.9	29	269.3	217.3	237
9/2 ..	1128.1	1128	1.2	1.2	2.8	14.1	24.6	18
11/2 ..	1282.5	1281	0.1	0.0		1.3	0.8	4
1/2 1/2 - [521] ..	936.5	936	15.3	15.2	15	279.9	279.5	364
3/2 ..	1027.9	1029	7.0	2.8	2.6	128.2	113.6	54
5/2 ..	1055.5	1056	5.1	4.3		86.0	87.1	66
7/2 ..	1268.2	1265	4.3	1.8		71.5	63.8	69
9/2 ..	1318.5	~ 1314	0.7	0.6		10.1	10.1	8
7/2 7/2 - [514] ..	1072.3	1072	2.0	3.8	16	40.3	81.5	91
9/2 ..	1218.6	1219	2.6	3.0	3	45.3	34.8	29
11/2 ..	1396.8	1397	0.0	0.1	< 3.6	0.8	1.3	15

^a See table 13.

^b The 7/2 1/2 - [510] state at 207 keV and the 3/2 3/2 - [512] state at 209 keV were not resolved. The experimental cross sections listed here and also used in figs. 28 and 29 were obtained by dividing the total observed cross section in the ratio indicated by the calculations.

TABLE 16. Comparison of unperturbed, Coriolis coupled and experimental cross sections in ^{185}W ($\theta = 90^\circ$).

State ^a	Energy (keV)		$\sigma(d,p)$ $\mu\text{b}/\text{sr}$			$\sigma(d,f)$ $\mu\text{b}/\text{sr}$		
	Per-turbed	Exper-imental	Unper-turbed	Per-turbed	Exper-imental	Unper-turbed	Per-turbed	Exper-imental
9/2 9/2 - [505] ..	789.0	789	66	61.6	25	3.3	3.9	10
7/2 7/2 - [503] ..	243.5	243.5	334.2	341.3	316	58.1	72.2	154
9/2 ..	391.0	390.9	6.4	10.2		1.0	2.1	~ 3
11/2 ..	571.2	~ 570	0.5	0.5	~ 5.6	0.1	0.2	1.4
3/2 3/2 - [512] ..	0.0	0.0	107.2	29.6	5	58.8	1.7	1
5/2 ..	67.9	66.1	194.8	247.3	301	97.2	173.2	207
7/2 ..	172.5	173.8	23.4	7.2	11	11.7	1.0	1.3
9/2 ..	305.4	302	4.7	6.5	11	2.1	4.5	11
11/2 ..	478.3	~ 478	0.2	0.1		0.1	0.0	~ 0.4
1/2 1/2 - [510] ..	23.6	23.6	0.2	0.2	4	0.3	0.9	2.7
3/2 ..	93.8	93.8	180.0	261.8	357	343.2	422.6	308
5/2 ..	188.2	188.2	52.7	0.3	~ 4	92.4	14.1	11
7/2 ..	335.7	334	18.0	36.5	104	31.6	54.8	99
9/2 ..	492.8	~ 492	1.8	0.0		2.7	0.1	~ 0.8
11/2 ..	717.6	706	0.1	0.2	5	0.2	0.4	4
5/2 5/2 - [512] ..	888.3	888	0.0	0.0	< 3	0.2	0.2	14
7/2 ..	986.1	986	16.9	7.7	32	268.2	208.1	206
9/2 ..	1113.8	~ 1118	1.2	1.1		14.1	24.2	~ 20 ^c
1/2 1/2 - [521] ..	1013.0	~ 1008	13.9	13.9	< 62	281.0	280.5	~ 266 ^b
3/2 ..	1105.8	1106	6.4	2.8		128.7	106.8	~ 43
5/2 ..	1118.0	~ 1118	4.7	3.8		86.4	88.7	~ 20 ^a
7/2 ..	1334.3	1335	3.9	1.6		71.8	59.7	~ 25
9/2 ..	1358.4	1361	0.5	0.6		10.1	10.3	11
7/2 7/2 - [514] ..	1058.3	1058.3	2.1	4.1	15	40.3	86.2	80
9/2 ..	1218.9	~ 1219	2.7	1.2		45.3	33.5	19

^a See table 13.

^b Intensity of 1/2 1/2 - [521] component estimated from 125° cross sections.

^c Unresolved doublet. Total observed cross section equals 40 μb .

TABLE 17. Comparison of unperturbed, Coriolis coupled and experimental cross section in ^{187}W ($\theta = 90^\circ$).

State ^a	Energy (keV)		$\sigma(d,p)$ $\mu\text{b}/\text{sr}$		
	Perturbed	Experimental	Unperturbed	Perturbed	Experimental
9/2 9/2 - [505]	598.2	598	62.5	43.9	23
7/2 7/2 - [503]	350.6	350.6	346.0	346.0	211
9/2	482.3		6.7	25.2	
3/2 3/2 - [512]	0.0	0.0	84.2	53.9	37
5/2	77.5	77.5	151.6	178.6	213
7/2	186.5		18.3	9.1	< 8
9/2	329.3	329	3.7	4.7	~ 5
1/2 1/2 - [510]	149.3	145.7	0.1	0.1	< 8
3/2	204.8	204.9	121.2	151.6	272
5/2	304.1	303.2	35.5	8.4	21
7/2	432.1	432.4	12.1	21.3	71
9/2	607.4				
11/2	805.7				

^a See table 13.

TABLE 18. Mixing amplitudes ($a_{in} \times 100$) calculated for the $1/2 -$ states.

$K^\pi[Nn_zA]$	A	E(keV)	1/2 - [510]	1/2 - [521]
1/2 - [510]	185	24	-100	+ 02
	183	0	-100	+ 02
	181	458	- 99	- 16
1/2 - [521]	185	1008	+ 02	+100
	183	936	+ 02	+100
	181	385	- 16	+ 99
	179	222	- 04	+100

TABLE 19. Mixing amplitudes ($a_{in} \times 100$) calculated for the
3/2 - states.

$K^\pi [Nn_z A]$	A	E(keV)	3/2 - [512]	1/2 - [510]	1/2 - [521]
3/2 - [512].....	187	0	- 99	- 16	
	185	0	+ 94	+ 33	+ 01
	183	209	- 99	+ 15	- 03
	181	726	-100	+ 05	+ 05
1/2 - [510].....	187	205	- 16	+ 99	
	185	94	+ 33	- 94	+ 05
	183	47	- 15	- 99	+ 03
	181	529	- 06	- 95	- 30
	179	689	- 03	-100	- 09
1/2 - [521].....	185	1106	- 03	+ 04	+100
	183	1029	- 03	+ 04	+100
	181	450	+ 04	- 30	+ 95
	179	305	+ 03	- 09	+100

TABLE 20. Mixing amplitudes ($a_{in} \times 100$) calculated for the
5/2 - states.

$K^\pi [Nn_z A]$	A	E(keV)	3/2 - [512]	1/2 - [510]	5/2 - [512]	1/2 - [521]
3/2 - [512].....	187	77	- 97	- 23		
	185	66	+ 91	+ 42	+ 00	+ 02
	183	292	+ 98	- 20	+ 00	+ 06
	181	807	-100	+ 06	+ 00	+ 07
1/2 - [510].....	187	303	- 23	+ 97		
	185	188	- 42	+ 90	- 00	- 08
	183	99	+ 20	+ 98	+ 00	- 05
	181	560	- 09	- 85	+ 00	- 52
	179	788	- 05	- 99	+ 00	- 11
5/2 - [512].....	185	888	- 00	+ 00	+100	- 00
	183	906	- 00	+ 00	+100	- 00
	181	366	- 00	- 00	-100	- 00
	179	430	- 00	+ 00	-100	+ 00
1/2 - [521].....	185	1118	- 05	+ 07	+ 00	+100
	183	1056	+ 05	- 06	- 00	-100
	181	488	+ 03	- 53	- 00	+ 85
	179	318	+ 04	- 12	+ 00	+ 99

TABLE 21. Mixing amplitudes ($a_{in} \times 100$) calculated for the $7/2^-$ states.

$K^\pi[Nn_zA]$	A	E(keV)	$7/2^-$ [503]	$3/2^-$ [512]	$1/2^-$ [510]	$5/2^-$ [512]	$1/2^-$ [521]	$7/2^-$ [514]
$7/2^-$ - [503].....	187	351	+100	+00	+00			
	185	244	+100	-00	-00	+ 05	+ 00	- 00
	183	453	+100	-00	+00	+ 05	- 00	- 00
	181	662	+ 98	-00	-00	- 19	- 00	- 03
$3/2^-$ - [512].....	187	(186)	+ 00	-95	-30	+ 00	+ 02	+ 00
	185	174	+ 00	+91	+42	+ 00	+ 02	+ 00
	183	412	- 00	-96	+26	- 00	- 08	+ 00
	181	937	- 00	-99	+10	+ 00	+ 13	+ 00
$1/2^-$ - [510].....	187	432	+ 00	-30	+95	- 00	- 11	+ 00
	185	334	+ 00	-41	+90	- 00	- 11	+ 00
	183	207	+ 00	+27	+96	+ 00	- 05	+ 00
	181	(730)	+ 00	+16	+79	- 00	+ 59	+ 00
$5/2^-$ - [512].....	185	986	- 05	-00	+00	+ 98	- 00	- 19
	183	1002	- 05	-00	+00	+ 98	- 00	- 17
	181	476	- 17	-00	-00	- 79	- 00	- 59
	179	532		-00	-00	-100	+ 00	- 07
$1/2^-$ - [521].....	185	1335	+ 00	+06	-09	- 00	- 99	+ 00
	183	1265	+ 00	+06	-07	- 00	-100	+ 00
	181	642	- 00	+04	-61	- 00	+ 79	+ 00
	179	508		+05	-20	+ 00	+ 98	+ 00
$7/2^-$ - [514].....	185	1058	+ 01	+00	+00	- 19	+ 00	- 98
	183	1072	+ 01	+00	+00	- 17	+ 00	- 99
	181	409	- 09	-00	-00	- 58	- 00	+ 81
	179	0		+00	+00	- 07	+ 00	+100

TABLE 22. Mixing amplitudes ($a_{in} \times 100$) calculated for the
9/2 - states.

$K^\pi [Nn_z A]$	A	E(keV)	9/2 - [505]	7/2 - [503]	3/2 - [512]	1/2 - [510]	5/2 - [512]	1/2 - [521]	7/2 - [514]
3/2 - [505]	187	598	- 95	- 33	+ 00	+ 00			
	185	789	- 100	- 07	+ 00	+ 00	- 01	+ 00	- 04
	183	1390	+ 100	+ 01	+ 00	+ 00	- 00	+ 00	- 04
7/2 - [503]	187	(482)	- 33	+ 95	+ 00	+ 00			
	185	391	- 07	+ 99	- 00	- 00	+ 08	+ 00	- 00
	183	595	- 01	+ 100	- 00	+ 00	+ 08	- 00	- 00
	181	(813)		- 97	+ 00	+ 00	+ 25	+ 00	+ 05
3/2 - [512]	187	329	+ 00	+ 00	+ 94	+ 34			
	185	302	+ 00	- 00	- 89	- 45	- 00	- 03	+ 00
	183	553	+ 00	- 00	- 96	+ 26	- 00	- 11	+ 00
1/2 - [510]	187		+ 00	+ 00	- 34	+ 94			
	185	492	- 00	+ 00	- 44	+ 88	- 00	- 15	+ 00
	183	309	+ 00	+ 00	- 27	- 96	- 00	+ 07	+ 00
5/2 - [512]	185	1118	+ 00	- 08	- 00	+ 00	+ 98	- 00	- 20
	183	1128	- 00	- 08	- 00	+ 00	+ 98	- 00	- 20
	181	~ 611		- 21	- 00	- 00	- 64	- 00	- 74
	179	(662)			- 00	- 00	- 99	+ 00	- 10
1/2 - [521]	185	1361	+ 00	+ 00	- 09	+ 13	+ 00	+ 99	+ 00
	183	1314	+ 00	+ 00	- 09	+ 09	+ 00	+ 99	+ 00
	181	(804)		+ 00	+ 15	+ 59	- 00	+ 79	- 00
	179				+ 06	- 20	+ 00	+ 98	+ 00
7/2 - [514]	185	1219	+ 04	+ 02	+ 00	+ 00	- 20	+ 00	- 98
	183	1219	- 04	+ 01	+ 00	+ 00	- 20	+ 00	- 98
	181	~ 527		- 15	- 00	- 00	- 72	- 00	+ 67
	179	120			- 00	+ 00	- 10	+ 00	+ 99

References

- 1) D. G. BURKE, B. ZEIDMAN, B. ELBEK, B. HERSKIND and M. OLESEN, *Mat. Fys. Medd., Dan. Vid. Selsk.*, **35** no. 2 (1966).
- 2) P. O. TJØM and B. ELBEK, *Mat. Fys. Medd., Dan. Vid. Selsk.*, **36** no. 8 (1967).
- 3) P. O. TJØM and B. ELBEK, *Mat. Fys. Medd., Dan. Vid. Selsk.*, **37** no. 7 (1969).
- 4) T. GROTDAL, K. NYBØ and B. ELBEK, *Mat. Fys. Medd., Dan. Vid. Selsk.*, **37** no. 12 (1970).
- 5) A. K. KERMAN, *Mat. Fys. Medd., Dan. Vid. Selsk.*, **30** no. 15 (1956).
- 6) R. J. BROCKMEIER, S. WAHLBORN, E. J. SEPPI and F. BOEHM, *Nucl. Phys.* **63** (1965) 102.
- 7) S. G. MALMSKOG and S. WAHLBORN, *Nucl. Phys. A* **102** (1967) 273.
- 8) P. G. HANSEN, P. HORNSHØJ and K. H. JOHANSEN, *Nucl. Phys. A* **126** (1969) 464.
- 9) S. A. HJORTH, H. RYDE, K. A. HAGEMANN, G. LØVHØIDEN and J. G. WADDINGTON, *Nucl. Phys.* **144** (1970) 513.
- 10) F. S. STEPHENS, M. D. HOLTZ, R. M. DIAMOND and J. O. NEWTON, *Nucl. Phys.* **115** (1968) 129.
- 11) P. KLEINHEINZ, R. F. CASTEN and B. NILSSON, *Nucl. Phys.* to be published.
- 12) J. R. ERSKINE, *Phys. Rev.* **138 B** (1965) 66.
- 13) R. H. SIEMSEN and J. R. ERSKINE, *Phys. Rev. Letters* **19** (1967) 70.
- 14) R. H. SIEMSEN and J. R. ERSKINE, *Phys. Rev.* **146** (1966) 911.
- 15) B. ELBEK and P. O. TJØM, *Advances in Nuclear Physics*, M. BARANGER and E. VOGT, Eds. (Plenum Press, New York 1969) vol. 3.
- 16) W. A. BONDARENKO and P. MANFRASS, *Zentralinstitut für Kernforschung, Rosendorf, Report no. 150, 1968 (unpubl.)* p. 67.
- 17) B. ELBEK, M. C. OLESEN and O. SKILBREID, *Nucl. Phys.* **10** (1959) 294.
- 18) P. R. CHRISTENSEN, A. BERINDE, I. NEAMU and N. SCINTEI, *Nucl. Phys. A* **129** (1969) 337.
- 19) C. M. PEREY and F. G. PEREY, *Phys. Rev.* **132** (1963) 755; F. G. PEREY, *Phys. Rev.* **131** (1963) 745.
- 20) M. JASKOLA, K. NYBØ, P. O. TJØM and B. ELBEK, *Nucl. Phys. A* **96** (1967) 52.
- 21) E. R. FLYNN, G. IGO, P. D. BARNES, R. F. CASTEN and J. R. ERSKINE, *Nucl. Phys. A* **159** (1970) 598.
- 22) J. H. E. MATTAUCH, W. THIELE and A. H. WAPSTRA, *Nucl. Phys.* **67** (1965) 1.
- 23) B. HARMATZ and T. H. HANDLEY, *Nucl. Phys. A* **121** (1968) 481.
- 24) P. J. DALY, K. AHLGREN, K. J. HOFSTETTER and R. HOCHÉL, *Nucl. Phys. A* **161** (1971) 177.
- 25) E. MOLL and U. GRUBER, *Z. Physik* **197** (1966) 113.

- 26) P. J. DALY, P. KLEINHEINZ and R. F. CASTEN, Nucl. Phys. A **123** (1969) 186.
- 27) T. KUROYANAGI and T. TAMURA, Nucl. Phys. A **133** (1969) 554.
- 28) Nuclear Data Sheets, compiled by K. WAY et al. (1959-1966).
- 29) L. V. GROSHV, A. M. DEMIDOV, V. I. PELEKHOV, L. L. SOKOLOVSKII, G. A. BARTHOLOMEW, A. DOVEIKA, K. M. EASTWOOD and S. MONARO, Nucl. Data A **5** (1969) 243.
- 30) H. H. BOLOTIN and D. A. McCLURE, in *Neutron Capture Gamma-Ray Spectroscopy* (IAEA, Vienna, 1969) p. 389.
- 31) H. SODAN, L. FUNKE, K.-H. KAUN, P. KEMNITZ and G. WINTER, Zentralinstitut für Kernforschung, Rossendorf, preprint (1969).
- 32) P. KLEINHEINZ and J. UNGRIN, unpublished data.
- 33) Chart of the Nuclides, 1968.
- 34) S. G. NILSSON, C. F. TSANG, A. SOBIEZEWSKI, Z. SZYMANSKI, S. WYCECH, C. GUSTAFSSON, I.-L. LAMM, P. MÖLLER and B. NILSSON, Nucl. Phys. A **131** (1969) 1.
- 35) B. ELBEK, M. KREGAR and P. VEDELSBY, Nucl. Phys. **86** (1966) 385.
- 36) D. L. HENDRIE, N. K. GLENDENNING, B. G. HARVEY, O. N. JARVIS, H. H. DUHM, J. SAUDINOS and J. MAHONEY, Phys. Letters **26 B** (1968) 127.
- 37) P. KLEINHEINZ, T. LINDBLAD and H. RYDE, to be published.
- 38) S. G. NILSSON, Mat. Fys. Medd., Dan. Vid. Selsk., **29** no. 16 (1955).
- 39) D. BREITIG, Z. Naturf., **26 a** (1971) 371.
- 40) J. P. SCHIFFER, P. KIENLE and G. C. MORRISON, Proc. Conf. Nucl. Isospin, Asilimar, March 1969, p. 679.
- 41) F. A. RICEY and R. K. SHELINE, Phys. Rev. **170** (1968) 1157.
- 42) C. SØNDERGAARD and B. S. NIELSEN, Physics Laboratory, Royal Vet. Univ. Copenhagen, private communication.
- 43) R. F. CASTEN, private communication.
- 44) B. L. ANDERSEN, Nucl. Phys. A **162** (1971) 208.
- 45) F. A. GAREEV, S. P. IVANOVA and V. V. PASHKEWITCH, Dubna Preprint E4-4704 (1969).
- 46) C. GÜNTHER, P. KLEINHEINZ, R. F. CASTEN and B. ELBEK, Nucl. Phys., A **172** (1971) 273.
- 47) R. F. CASTEN, P. KLEINHEINZ, P. J. DALY and B. ELBEK, Phys. Rev. **03** (1971) 1271.
- 48) C. GUSTAFSSON, I.-L. LAMM, B. NILSSON and S. G. NILSSON, Arkiv för Fysik **36** (1967) 613.
- 49) G. LØVHØIDEN, J. C. WADDINGTON, K. A. HAGEMANN, S. A. HJORTH and H. RYDE, Nucl. Phys. A **148** (1970) 657.
- 50) B. L. ANDERSEN, B. SØRENSEN, B. MOTTELSON and G. E. BROWN, Wednesday Circus, Niels Bohr Institute, March 1971.



